

Communication-Efficient Federated Learning Using Censored Heavy Ball Descent

Yicheng Chen, Rick S. Blum, *Fellow, IEEE*, and Brian M. Sadler, *Life Fellow, IEEE*

Abstract—Distributed machine learning enables scalability and computational offloading, but requires significant levels of communication. Consequently, communication efficiency in distributed learning settings is an important consideration, especially when the communications are wireless and battery-driven devices are employed. In this paper we develop a censoring-based heavy ball (CHB) method for distributed learning in a server-worker architecture. Each worker self-censors unless its local gradient is sufficiently different from the previously transmitted one. The significant practical advantages of the HB method for learning problems are well known, but the question of reducing communications has not been addressed. CHB takes advantage of the HB smoothing to eliminate reporting small changes, and provably achieves a linear convergence rate equivalent to that of the classical HB method for smooth and strongly convex objective functions. The convergence guarantee of CHB is theoretically justified for both convex and nonconvex cases. In addition we prove that, under some conditions, at least half of all communications can be eliminated without any impact on convergence rate. Extensive numerical results validate the communication efficiency of CHB on both synthetic and real datasets, for convex, nonconvex, and nondifferentiable cases. Given a target accuracy, CHB can significantly reduce the number of communications compared to existing algorithms, achieving the same accuracy without slowing down the optimization process.

Index Terms—Censoring, communication-efficient, federated learning, heavy ball.

I. INTRODUCTION

Traditional centralized optimization algorithms for machine learning applications have a number of limitations when applied in networked settings. This is especially clear in some applications where abundant distributed processing resources are inherently available such as vehicular, mobile cellular, and sensor networks. This motivates distributed optimization that balances communications and processing. One popular distributed optimization problem can be formulated as

$$\min_{\theta \in \mathbb{R}^d} f(\theta) \quad \text{with} \quad f(\theta) \triangleq \sum_{m \in \mathcal{M}} f_m(\theta) \quad (1)$$

where $\theta \in \mathbb{R}^d$ is the model parameter vector to be optimized, $f(\theta)$ is the objective function to be minimized, and $f_m(\theta)$ is the local function for worker $m \in \mathcal{M} = \{1, 2, \dots, M\}$. The

The work was supported by the U. S. Army Research Laboratory and the U. S. Army Research Office under grant number W911NF-17-1-0331 and by the Office of Naval Research grant number N00014-22-1-2626.

Yicheng Chen is with Reality Labs Meta, Redmond, WA 98052 USA (email: chenggejiayou@gmail.com).

Rick S. Blum is with Lehigh University, Bethlehem, PA 18015 USA (email: rblum@eecs.lehigh.edu).

Brian M. Sadler is with DEVCOM ARL, Adelphi, MD 20878 USA (email: brian.m.sadler6.civ@mail.mil).

problem in (1) has been successfully applied as a model in multi-agent systems [1]–[3], sensor networks [4]–[8], smart grids [9], and distributed learning [10]–[13]. To relate (1) to a distributed learning setting, let $f_m(\theta) \triangleq \sum_{n=1}^{N_m} \ell(\theta; \mathbf{x}_n, y_n)$ denote the loss function $\ell(\theta; \mathbf{x}_n, y_n)$ summed over all the training data $\{(\mathbf{x}_n, y_n), n = 1, 2, \dots, N_m\}$ at worker/node m , where \mathbf{x}_n is the n -th feature vector and y_n is the corresponding label. A common method to solve (1) uses a worker-server architecture where a central server updates the model parameter by aggregating the gradients computed at all workers and then transmits the updated parameter back to the workers. The learning task is solved after many communications between workers and the server. However, the communications latency is generally orders of magnitude larger than local memory access, e.g., about 2500 times larger over a standard network connection [14]. For this reason, the required communications can be a significant bottleneck on overall performance, especially in federated learning and edge AI systems [15]–[22]. The communications can also be a large drain on the batteries of mobile nodes. Therefore, it is extremely important to develop distributed optimization algorithms that are efficient in terms of communications. In this paper we develop a communication-efficient server-worker processing scheme to significantly reduce communications without sacrificing convergence speed.

A. Prior Art

The challenge of communication-efficient distributed optimization has been addressed in several ways. Data compression is one popular solution to reduce the bandwidth usage per transmission. The existing approaches mainly exploit quantization and sparsification. Quantization aims to approximate a continuous-valued quantity using a finite set of values to simplify processing and storage, and has been successfully applied in many distributed optimization algorithms [18], [23]–[28]. Sparsification techniques can also reduce bandwidth. For example some small gradient vector coordinates can be assumed to be zero while the remaining coordinates can be appropriately amplified to ensure the sparsified gradient is unbiased [17], [29]–[31]. However, the existing efforts for quantization and sparsification reduce the bandwidth usage, not the number of communications. Additionally, quantization and sparsification bring noise and errors which slow down the optimization process in general.

In addition to reducing the number of bits per communication, accelerating convergence is another straightforward method to enhance communication efficiency. One-shot parameter

averaging methods were proposed in [32]–[35] to find the optimal minimizer using only one iteration. While the idea of reducing the number of iterations is desirable, one-iteration approaches may sacrifice too much performance to accomplish this goal in some cases [36]. As an alternative to summing gradients, researchers have considered more sophisticated methods where a worker can compute (or approximately compute) its local Hessian. Examples of these approaches include quasi-Newton methods [37]–[41] and approximated Newton methods [36], [42], [43]. On the other hand, primal-dual methods [14], [44]–[46] are also shown to be efficient in distributed optimization where the primal solution is obtained by solving the dual problem. However, these algorithms save communications at the cost of increasing local computation, unlike the method proposed in this paper which does not increase local computation compared to the first-order algorithms where only the local gradient is computed.

As an alternative to speeding up the optimization process, reducing the number of transmissions per iteration is another efficient way to save communications. An approach called censoring has previously been studied for applications other than learning [47]–[50]. Censoring eliminates transmissions of less informative data, thus reducing worker communications. The original work [47]–[50] focused on hypothesis testing and the censoring was applied to the worker likelihood ratios. Later, the ideas were applied to distributed optimization, where the censoring was applied to workers such that worker gradients are not transmitted if they do not change significantly compared to previously transmitted ones. Distributed optimization approaches employing censoring include the event-triggered zero-gradient-sum algorithms [51], and the censoring-based subgradient algorithm [52]. However, the step size of the algorithms in [51], [52] is reduced at each iteration to guarantee convergence, which results in relatively slow progress in the optimization process as the step size becomes smaller and smaller. Distributed dual averaging with censoring was proposed in [53] but it does not have theoretical justification for convergence or communication saving, unlike this paper. Gradient descent (GD) with censoring was proposed in [54] to save communications for machine learning in a comprehensive study that our paper builds upon. In [54], each step is chosen according to the approximated steepest descent direction without considering previous search directions, whereas in our paper we propose a heavy ball (HB) method with a momentum term. The significant practical advantages of the HB method for learning problems are well known [55], [56], but the question of reducing communications, including convergence, has not been addressed. The following proposed censoring-based heavy ball (CHB) method accelerates convergence, as might be expected from previous studies of heavy ball, but also takes advantage of the momentum term to smooth the gradient and reduce changes resulting in further communication savings.

Our contributions. In this paper we develop a censoring-based heavy ball (CHB) method for distributed learning in the server-worker architecture where our censoring threshold for each worker to decide whether to transmit or not at each iteration is proposed in an intuitive and straightforward way. Combining the censoring threshold with the CHB parameter

update rule, a rigorous convergence guarantee is derived in this paper for CHB under strongly convex, convex and nonconvex cases. Our results also demonstrate that CHB can achieve the same linear convergence rate as the classical HB method for a smooth and strongly convex objective function. We show that more than half of the communications can be saved without any impact on the convergence rate under certain conditions. Numerical experimental results demonstrate that CHB is able to significantly reduce the total number of communications while maintaining a fast convergence rate to a target solution accuracy when compared to other distributed learning algorithms for both synthetic and real datasets.

Notation. Bold lower case letters are used throughout this paper to denote column vectors. The notation $\|\mathbf{x}\|$ and \mathbf{x}^\top is employed to denote the ℓ_2 -norm and the transpose of a column vector \mathbf{x} , respectively.

II. CENSORING-BASED HEAVY BALL METHOD

Before introducing our method for reducing communications, we begin with a brief discussion of the classical HB method [57], a popular iterative optimization algorithm, and focus on its parameter update rule in a distributed system with a server and M workers. Specifically, at iteration k of HB, the server broadcasts the current parameter $\boldsymbol{\theta}^k$ to all workers; each worker m computes the gradient $\nabla f_m(\boldsymbol{\theta}^k)$ based on its own local function $f_m(\boldsymbol{\theta}^k)$ and transmits $\nabla f_m(\boldsymbol{\theta}^k)$ back to the server. Upon receiving $\nabla f_m(\boldsymbol{\theta}^k)$ from each worker, the server updates $\boldsymbol{\theta}^k$ as [57]

$$\begin{aligned} \text{HB-update} \quad \boldsymbol{\theta}^{k+1} &= \boldsymbol{\theta}^k - \alpha \nabla f(\boldsymbol{\theta}^k) + \beta(\boldsymbol{\theta}^k - \boldsymbol{\theta}^{k-1}) \text{ with} \\ \nabla f(\boldsymbol{\theta}^k) &\triangleq \sum_{m \in \mathcal{M}} \nabla f_m(\boldsymbol{\theta}^k) \end{aligned} \quad (2)$$

where α is the step size, β is a constant, and $\nabla f(\boldsymbol{\theta}^k)$ is the gradient of $f(\boldsymbol{\theta}^k)$. To implement (2) requires M communications from the workers to the server during each iteration k .

Our communication-efficient CHB algorithm will be described next. Each worker maintains two vectors concerning iteration k . One is the parameter vector $\boldsymbol{\theta}^k$ sent by the server at the start of iteration k . The other is the last gradient $\nabla f_m(\hat{\boldsymbol{\theta}}_m^{k-1})$ transmitted from worker m to the server prior to iteration k . An important feature of CHB is that a worker m will not transmit to the server if the current gradient $\nabla f_m(\boldsymbol{\theta}^k)$ is not sufficiently different from the previously transmitted gradient $\nabla f_m(\hat{\boldsymbol{\theta}}_m^{k-1})$. Define

$$\delta \nabla_m^k \triangleq \nabla f_m(\boldsymbol{\theta}^k) - \nabla f_m(\hat{\boldsymbol{\theta}}_m^{k-1}). \quad (3)$$

It is worth mentioning that $\delta \nabla_m^k$ characterizes the “newness” of the information contained in the gradient of worker m at iteration k . To implement the CHB algorithm, at the beginning of iteration k the server broadcasts $\boldsymbol{\theta}^k$ to all workers. Then only if worker m has a gradient which is sufficiently different from that previously transmitted will it transmit $\delta \nabla_m^k$ back to the server. Immediately after transmitting, worker m will update its transmitted gradient $\nabla f_m(\hat{\boldsymbol{\theta}}_m^k) = \nabla f_m(\boldsymbol{\theta}^k)$ while others keep their previous values $\nabla f_m(\hat{\boldsymbol{\theta}}_m^k) = \nabla f_m(\hat{\boldsymbol{\theta}}_m^{k-1})$.

At the end of iteration k , the server updates the parameter θ via

CHB-update $\theta^{k+1} = \theta^k - \alpha \nabla^k + \beta(\theta^k - \theta^{k-1})$ with

$$\nabla^k \triangleq \sum_{m \in \mathcal{M}^k} \nabla f_m(\hat{\theta}^k) \quad (4)$$

where ∇^k is an approximation to the gradient at iteration k which is computed recursively using

$$\nabla^k = \nabla^{k-1} + \sum_{m \in \mathcal{M}^k} \delta \nabla_m^k. \quad (5)$$

Here \mathcal{M}^k is a set which collects the indices of workers who have transmitted during iteration k and whose cardinality is denoted $|\mathcal{M}^k|$. The number of communications are often reduced to $|\mathcal{M}^k| < M$ during iteration k in the CHB algorithm which explains the term $\sum_{m \in \mathcal{M}^k} \delta \nabla_m^k$ in (5). In fact, if we replace \mathcal{M}^k in (5) with \mathcal{M} , plugging (5) into (4) yields the classical HB update rule in (2).

Next we describe when a worker will skip a transmission, which we call the CHB-skip-transmission condition. To make the principles behind the design of the CHB-skip-transmission condition clear, the CHB update rule in (4) can be rewritten as

$$\theta^{k+1} = \theta^k - \alpha \left(\nabla f(\theta^k) - \sum_{m \in \mathcal{M}_c^k} \delta \nabla_m^k \right) + \beta(\theta^k - \theta^{k-1}) \quad (6)$$

$$= \theta^k - \alpha \nabla f(\theta^k) + \beta(\theta^k - \theta^{k-1}) + \alpha \sum_{m \in \mathcal{M}_c^k} \delta \nabla_m^k \quad (7)$$

where \mathcal{M}_c^k is a set which collects the indices of workers who do not transmit during iteration k , and $\delta \nabla_m^k$ is defined in (3). It is well known [57] that the update steps in HB tend to accumulate contributions in directions of persistent descent while canceling directions that oscillate. This interpretation provides some intuitive explanation as to why the HB method often outperforms gradient descent (GD) [57]. Since the update rule of CHB in (4) is very similar to that of the traditional HB method (just drop less informative terms), it is not surprising that we have observed that the CHB algorithm inherits the advantages from the HB method. Compared with the classical HB update rule in (2), the result in (7) shows that we can save transmissions by not allowing the workers in \mathcal{M}_c^k to transmit if $\delta \nabla_m^k$ for all $m \in \mathcal{M}_c^k$ is very small compared to $(\theta^k - \theta^{k-1})$. This takes advantage of the HB smoothing and as will see, we can save transmissions with very little affect on the optimization convergence rate. Therefore, the rule to determine if worker m will or will not transmit is called the **CHB-skip-transmission condition**,

$$\|\delta \nabla_m^k\|^2 \leq \varepsilon_1 \|\theta^k - \theta^{k-1}\|^2 \quad (8)$$

where ε_1 is a positive constant that allows us to tune the convergence while saving communications. Intuitively, smaller ε_1 leads to less communication censoring, e.g., CHB reduces to the classical HB method when we set $\varepsilon_1 = 0$. On the other hand, when ε_1 increases, the number of communications per iteration is reduced at the cost of increasing the number of iterations. A favorable communication-iteration trade-off can be achieved by CHB via tuning ε_1 ; see the example in Figure 11. Finding a theoretically optimal value of ε_1 is an interesting

open problem. Note that using similar steps to those shown in [54], the condition (8) can also be derived based on the criterion which ensures that CHB has larger per-communication descent than HB. At iteration k , after receiving θ^k from the server, each worker can independently check the CHB-skip-transmission condition (8). If the CHB-skip-transmission condition is not satisfied, then worker m will immediately transmit $\delta \nabla_m^k$ to the server. The CHB algorithm is summarized as Algorithm 1.

Algorithm 1 CHB

Input: step size α , positive constants ε_1 and β .
Initialize: $\theta^1, \{\nabla \mathcal{L}_m(\hat{\theta}_m^0), \forall m\}$

- 1: **for** $k = 1, 2, \dots, K$ **do**
- 2: Server broadcasts θ^k at the starting time of iteration k .
- 3: **for** $m = 1, 2, \dots, M$ **do**
- 4: **if** the CHB-skip-transmission condition in (8) is not satisfied for worker m **then**
- 5: Worker m transmits $\delta \nabla_m^k$ to the server and locally updates $\nabla f_m(\hat{\theta}_m^k) = \nabla f_m(\theta^k)$.
- 6: **else**
- 7: Worker m does not transmit but locally updates $\nabla f_m(\hat{\theta}_m^k) = \nabla f_m(\hat{\theta}_m^{k-1})$.
- 8: **end if**
- 9: **end for**
- 10: Server updates θ^k via (4).
- 11: **end for**

III. CONVERGENCE AND COMMUNICATION ANALYSIS

In this section, convergence rate and communication reduction guarantees for CHB are developed for the proper choice of the constants α , β , and ε_1 . The following assumptions and definitions are needed for the provided results.

Assumption 1. *In (1), $f(\theta)$ is L -smooth and coercive. This implies there exists a constant $L > 0$ such that $\|\nabla f(\theta_1) - \nabla f(\theta_2)\| \leq L\|\theta_1 - \theta_2\|$, $\forall \theta_1, \theta_2$ [58] and $\lim_{\|\theta\| \rightarrow \infty} f(\theta) = +\infty$ [59].*

Definition 1. *The objective function $f(\theta)$ in (1) is μ -strongly convex, which implies the existence of a constant $\mu > 0$ such that $f(\theta_1) \geq f(\theta_2) + \nabla f(\theta_2)^\top(\theta_1 - \theta_2) + \frac{\mu}{2}\|\theta_1 - \theta_2\|^2$, $\forall \theta_1, \theta_2$ [58].*

Definition 2. *The objective function $f(\theta)$ in (1) is convex, which implies $f(\theta)$ satisfies $f(\lambda\theta_1 + (1 - \lambda)\theta_2) \leq \lambda f(\theta_1) + (1 - \lambda)f(\theta_2)$, $\forall \theta_1, \theta_2$ and $0 \leq \lambda \leq 1$ [59].*

Assumption 2. *In (1), $f_m(\theta)$ is L_m -smooth for each worker m . This implies there exists a constant $L_m > 0$ such that $\|\nabla f_m(\theta_1) - \nabla f_m(\theta_2)\| \leq L_m\|\theta_1 - \theta_2\|$, $\forall \theta_1, \theta_2$ [58].*

Let

$$\mathbb{L}(\theta^k) \triangleq f(\theta^k) - f(\theta^*) + \eta_1 \|\theta^k - \theta^{k-1}\|^2 \quad (9)$$

define a Lyapunov function, where θ^* is the optimal solution to the optimization problem in (1), and η_1 is a non-negative constant. If we allow all workers to transmit ($\mathcal{M}^k = \mathcal{M}$) and set $\eta_1 = 0$, then CHB reduces to the classical HB method and $\mathbb{L}(\theta^k)$ will describe the optimization process of the HB

method. However, when some communications are suppressed, the following lemma describes the behavior of the Lyapunov function defined in (9).

Lemma 1. *Under Assumption 1, if the constants α , β , and ε_1 are chosen so that*

$$\sigma_0 \geq 0 \text{ with } \sigma_0 \triangleq \frac{\alpha}{2} - \left(\eta_1 - \frac{1 - \alpha L}{2\alpha} \right) \alpha^2 (1 + \rho_1) (1 + \rho_2), \quad (10)$$

$$\begin{aligned} \sigma_1 \geq 0 \text{ with } \sigma_1 \triangleq -\gamma |\mathcal{M}_c^k|^2 \varepsilon_1 - \frac{\beta^2}{2\alpha} (1 + \rho_3^{-1}) \\ - \left(\eta_1 - \frac{1 - \alpha L}{2\alpha} \right) \beta^2 (1 + \rho_1^{-1}) + \eta_1, \end{aligned} \quad (11)$$

$$\begin{aligned} \gamma \geq \frac{\alpha}{2} (1 + \rho_3) \text{ with } \gamma \triangleq \frac{\alpha}{2} (1 + \rho_3) \\ + \left(\eta_1 - \frac{1 - \alpha L}{2\alpha} \right) \alpha^2 (1 + \rho_1) (1 + \rho_2^{-1}), \end{aligned} \quad (12)$$

where η_1 is the non-negative constant in (9), $|\mathcal{M}_c^k|$ is the cardinality of \mathcal{M}_c^k , and $\rho_1, \rho_2, \rho_3 > 0$, then the Lyapunov function follows

$$\mathbb{L}(\boldsymbol{\theta}^{k+1}) - \mathbb{L}(\boldsymbol{\theta}^k) \leq -\sigma_0 \|\nabla f(\boldsymbol{\theta}^k)\|^2 - \sigma_1 \|\boldsymbol{\theta}^k - \boldsymbol{\theta}^{k-1}\|^2 \quad (13)$$

where constants $\sigma_0 \geq 0$ and $\sigma_1 \geq 0$ depend on α , β and ε_1 . The result in (13) implies $\mathbb{L}(\boldsymbol{\theta}^{k+1}) \leq \mathbb{L}(\boldsymbol{\theta}^k)$. \blacksquare

Proof: Please refer to Appendix B. \blacksquare

From (11), we know that $\sigma_1 = \sigma_1(|\mathcal{M}_c^k|)$ but for simplicity, we omit $|\mathcal{M}_c^k|$ here. Note that if we set $(\eta_1 - \frac{1 - \alpha L}{2\alpha}) = 0$, then (10)–(12) are equivalent to

$$\begin{aligned} \alpha \leq \frac{1}{L}, \quad \beta \leq \sqrt{\frac{1 - \alpha L}{1 + \rho_3^{-1}}}, \quad \text{and} \\ \varepsilon_1 \leq \frac{(1 - \alpha L) - \beta^2 (1 + \rho_3^{-1})}{\alpha^2 (1 + \rho_3) |\mathcal{M}_c^k|^2}. \end{aligned} \quad (14)$$

It can be shown that (14) admits an uncountable number of solutions for α , β and ε_1 which would guarantee (10)–(12). Some examples of other parameter choices can be found at the end of Appendix B. Next, we will show that the Lyapunov function in (9) has a linear convergence rate under certain conditions.

Theorem 1. (strongly convex) *Under Assumption 1 and Definition 1, if constants α , β and ε_1 are properly selected such that (10)–(12) are satisfied with $\sigma_0 > 0$ in (10) and $\sigma_1 > 0$ in (11), then the Lyapunov function in (9) converges Q -linearly; that is, there exists a constant $c(\alpha, \beta, \varepsilon_1) \in (0, 1)$ such that at iteration k ,*

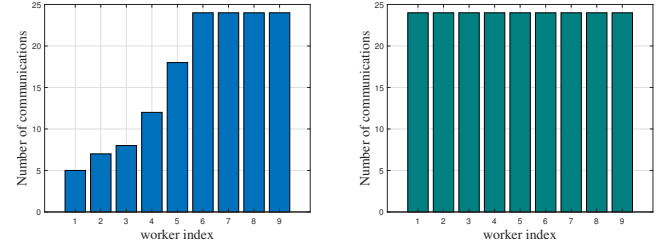
$$\mathbb{L}(\boldsymbol{\theta}^{k+1}) \leq (1 - c(\alpha, \beta, \varepsilon_1)) \mathbb{L}(\boldsymbol{\theta}^k) \quad (15)$$

where $c(\alpha, \beta, \varepsilon_1) = \min \{2\sigma_0\mu, \min_k \{\sigma_1\}/\eta_1\}$ with σ_0 and σ_1 defined in (10) and (11), respectively. The result in (15) implies

$$f(\boldsymbol{\theta}^k) - f(\boldsymbol{\theta}^*) \leq (1 - c(\alpha, \beta, \varepsilon_1))^k \mathbb{L}(\boldsymbol{\theta}^0). \quad (16)$$

Proof: Please refer to Appendix C. \blacksquare

Theorem 1 implies CHB can achieve a linear convergence rate which is of the same order as that for HB [60] under



(a) Comm. of 9 workers in CHB. (b) Comm. of 9 workers in HB.

Fig. 1: Number of communications of different workers for the first 24 iterations of CHB and HB in linear regression with $\alpha = 1/L$, $\varepsilon_1 = 0.1/(\alpha^2 M^2)$ and smoothness constants satisfying $L_1 < L_2 < \dots < L_9$ with $L_m = (1.3^{m-1})^2$.

Assumption 1 and Definition 1. If we set $\rho_3 = 1$, $\delta \in (0, 1)$, $\alpha = \frac{1-\delta}{L}$, $\eta_1 = \frac{1-\alpha L}{2\alpha}$, $\varepsilon_1 = \frac{(1-\alpha L)(1-\alpha\mu)}{4\alpha^2 M^2}$, and $\beta = \frac{1}{2}\sqrt{(1-\alpha L)(1-\alpha\mu)}$, then

$$c(\alpha, \beta, \varepsilon_1) = \frac{1-\delta}{L/\mu}, \quad (17)$$

which is exactly the same value we obtain in HB if we also choose $\alpha = (1-\delta)/L$ [60]. There are an uncountable number of other parameter settings in CHB that provide the same order convergence rate as HB. However, the just predicted theoretical convergence rates of CHB and HB are very conservative compared to what is observed in numerical examples. Numerical results in Section IV indicate that CHB with $\alpha = 1/L$ and $\beta > 0$ typically requires almost the same number of iterations as HB to achieve the same value of the left-hand-side of (16) and often outperforms GD. Convergence guarantees for CHB under general convex and nonconvex objective function cases are given next. The proofs are provided in Appendix D and Appendix E respectively.

Theorem 2. (convex) *Under Assumption 1 and Definition 2, if the constants α , β , and ε_1 are chosen so that (10)–(12) are satisfied with $\sigma_0 > 0$ in (10) and $\sigma_1 > 0$ in (11), then*

$$f(\boldsymbol{\theta}^k) - f(\boldsymbol{\theta}^*) = \mathcal{O}(1/k). \quad (18)$$

For nonconvex objective functions, the following convergence guarantee can be established.

Theorem 3. (nonconvex) *Under Assumption 1, if the constants α , β , and ε_1 are chosen so that (10)–(12) are satisfied with $\sigma_0 > 0$ in (10) and $\sigma_1 > 0$ in (11), then*

$$\lim_{k \rightarrow \infty} \|\nabla f(\boldsymbol{\theta}^k)\|^2 \rightarrow 0. \quad (19)$$

The following lemma illustrates a communication saving bound for the CHB algorithm. As indicated in Figure 1, worker m with a small smoothness constant L_m tends to transmit less frequently. The following lemma formally describes the impact of L_m on the communication savings of worker m .

Lemma 2. *Under Assumption 2, if the smoothness constant L_m of worker m satisfies*

$$L_m^2 \leq \varepsilon_1, \quad (20)$$

then after iteration k in CHB, the number of communications between worker m and the server, denoted as S_m , can be upper bounded by

$$S_m \leq \frac{k}{2}. \quad (21)$$

Proof: Please refer to Appendix F. \blacksquare

The result in Lemma 2 indicates the smoothness of the local function decides the number of communications needed by worker m . It makes sense that worker m with a small smoothness constant L_m tends to transmit less frequently because L_m indicates the maximum rate of change of worker m 's gradient. It is worth mentioning that if (20) is true for all workers and the conditions in (10)–(12) are satisfied with $\sigma_0 > 0$ in (10) and $\sigma_1 > 0$ in (11), then we can save at least half of the transmissions but we still achieve the same convergence rate as HB, which is known to be good.

IV. NUMERICAL EXPERIMENTS

To validate the theoretical results on convergence analysis and communication savings, the empirical performance of CHB is evaluated for (1) linear regression (convex), (2) regularized logistic regression (strongly convex), (3) lasso regression (nondifferentiable) and (4) training a neural network (nonconvex). The objective error $f(\boldsymbol{\theta}^k) - f(\boldsymbol{\theta}^*)$ evaluates the algorithm progress for linear regression, regularized logistic regression, and lasso regression. For training a neural network with one hidden layer with 30 nodes and the sigmoid activation function, we use the norm of the gradient $\|\nabla^k\|$ as a figure of merit of the progress. We consider a scenario with one server and nine workers. To benchmark CHB, we compare its performance with GD [58], censoring-based GD (called LAG-WK) [54], and the classical HB method [57] using synthetic datasets and real datasets. Except as stated elsewhere, we set the constant $\beta = 0.4$ for HB and CHB and choose the same skip-transmission condition (8) for CHB and censoring-based GD. Note that hereafter in the paper we refer to regularized logistic regression as logistic regression. The specific loss function formats of the above machine learning tasks can be found in [61]. For clarity of presentation, we divide the experiments into two sets.

A. Experiment Set 1

Synthetic dataset tests. Let us initially consider the impact of the smoothness constant on communication savings in synthetic datasets for linear regression and logistic regression. Specifically, we consider linear regression with increasing smoothness constants $L_m = (1.3^{m-1})^2$ for $m = 1, 2, \dots, 9$ in Figure 2 (same setting as Figure 1) and logistic regression with common smoothness constants $L_1 = L_2 = \dots = L_9 = 4$ in Figure 3. For these two cases, we randomly generate an independent sequence of labels (over n), each with equal probability of $y_n = 1$ or $y_n = -1$ for each worker m . Then we randomly generate 50 independent instances $\mathbf{x}_n \in \mathbb{R}^{50}$ (to pair with the labels) from a standard normal distribution and use the same approach as [54] to rescale the data to change the value of smoothness constants. To enable useful comparison,

we set $\alpha = 1/L$ for all algorithms. For censoring-based GD and CHB, we choose $\varepsilon_1 = 0.1/(\alpha^2 M^2)$ in (8). In Figure 2, it is not surprising that CHB requires a fewer number of communications compared to HB since we know from Figure 1 that workers with smaller smoothness constants tend to transmit less frequently such that communications can be saved for these workers. Interestingly, Figure 3 indicates that even when workers have the same smoothness constants, CHB can still save communications. Both Figure 2 and Figure 3 indicate CHB outperforms the alternatives in terms of the number of communications saved while still employing nearly the same number of iterations as HB to achieve the same objective error. In these cases, CHB requires not only a smaller number of communications but also a smaller number of iterations, compared to censoring-based GD, to attain the same objective error, .

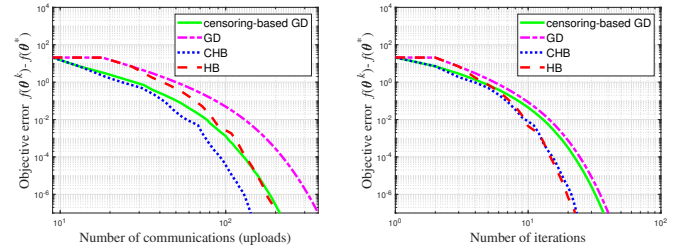


Fig. 2: Objective error versus the number of communications and iterations for linear regression with increasing smoothness constant $L_m = (1.3^{m-1})^2$ for $m = 1, 2, \dots, 9$ in synthetic datasets.

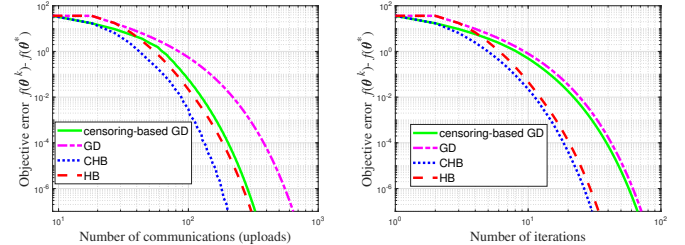


Fig. 3: Objective error versus the number of communications and iterations for logistic regression with common smoothness constants $L_1 = L_2 = \dots = L_9 = 4$ in synthetic datasets.

Real dataset tests. We also test the performance on the real dataset *ijcnn1* [62] which has 49990 samples and 22 features per sample. All samples are evenly split between nine workers. In addition to linear regression and logistic regression, we also consider lasso regression where we employ a subgradient to replace the gradient. In each of these three regression tasks, we set $\alpha = 10^{-4}$ for HB, CHB, GD and censoring-based GD. For CHB and censoring-based GD, we choose $\varepsilon_1 = 0.1/(\alpha^2 M^2)$. We set the regularization parameter to $\lambda = 0.001$ and $\lambda = 0.5$ for logistic regression and lasso regression, respectively. We stop the training process when the objective error $f(\boldsymbol{\theta}^k) - f(\boldsymbol{\theta}^*)$ is less than $10^{-7}, 10^{-5}, 10^{-7}$ for linear regression, logistic regression, and lasso regression, respectively. Figure 4 indicates that given a target accuracy, the

TABLE I: Performance comparison for the *ijcnn1* dataset. The objective error is 10^{-7} , 10^{-7} and 10^{-5} for linear regression, lasso regression and logistic regression, respectively. The fixed number of iterations for training a neural network is 500.

Name	Linear regression		Lasso regression		Logistic regression		Neural network	
	Comm.	Iter.	Comm.	Iter.	Comm.	Iter.	Comm.	Norm square grad.
CHB	465	109	424	108	546	5324	1083	6.2402×10^{-6}
HB	1071	119	1071	119	53244	5916	4500	6.3354×10^{-6}
LAG	799	203	608	197	864	9248	1361	3.7549×10^{-5}
GD	1917	213	1899	211	88866	9874	4500	3.7885×10^{-5}

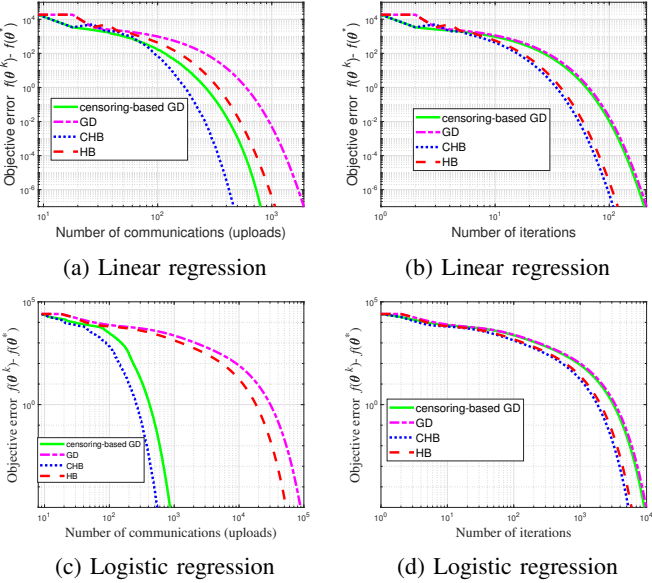


Fig. 4: Objective error versus the number of communications and iterations for linear regression and logistic regression in the *ijcnn1* dataset.

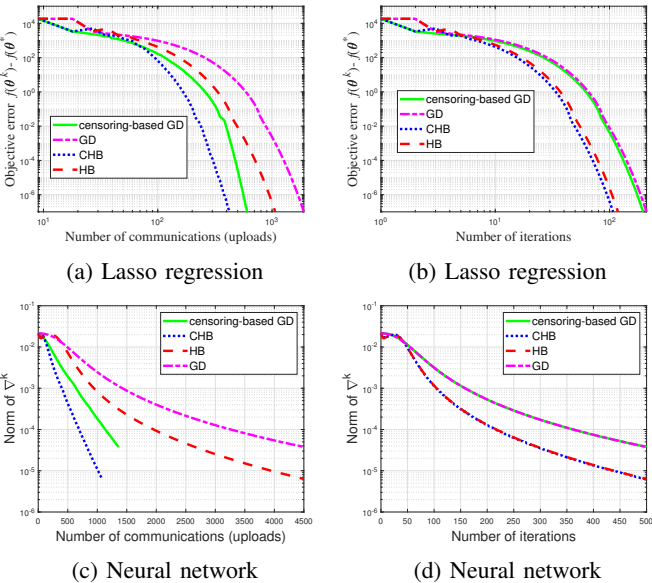


Fig. 5: Objective error versus the number of communications and iterations for lasso regression and training a neural network in the *ijcnn1* dataset.

number of iterations needed for CHB is almost the same as that for HB for linear regression and logistic regression, and it also verifies that CHB requires a smaller number of communications than the other methods. Even for the nondifferentiable lasso regression task, the variant of CHB shows similar performance in Figure 5(a) and Figure 5(b) as in linear regression and logistic regression. In all regression tasks, CHB reduces the communications compared to HB, by up to several orders of magnitude.

We also evaluate the performance of CHB for training a relatively small neural network with one hidden layer with 30 nodes. For training the neural network, all algorithms are stopped after 500 iterations with the step size $\alpha = 0.02$ while employing the regularization parameter $\lambda = 1/49990$. For CHB and censoring-based GD, we choose $\varepsilon_1 = 0.01$. Compared to HB, GD, and censoring-based GD, Figure 5(c) and Figure 5(d) illustrate that CHB has competitive convergence performance for this nonconvex problem with the smallest number of communications. Table I summarizes the number of communications and iterations to attain a given objective error which indicates the desirable performance of CHB in terms of communication savings and convergence rate. For linear and lasso regression, CHB reduces the communications to less than half that needed for HB, and for logistic regression the communications are reduced by two orders of magnitude compared to HB. For the neural network training example, CHB and HB reduce the norm square of the gradient by an order of magnitude compared to censoring-based GD and GD, and CHB uses only 24% of the communications needed for HB. Additional numerical results on other real datasets and discussion of the impact of step size are given next.

B. Experiment Set 2

To promote comparison, we first use the same real datasets with the same setup as [54]. Specifically, we consider linear regression with the *Housing*, *Body fat*, and *Abalone* datasets and logistic regression with the *Ionosphere*, *Adult fat*, and *Derm* datasets. We evenly split each dataset into three workers and employ the minimal number of features among all datasets as the number of features used in the test. Additionally, we also consider lasso regression with the *Ionosphere*, *Adult fat*, and *Derm* datasets. In all these regression tasks, we choose $\alpha = 1/L$ for all four algorithms. For CHB and censoring-based GD, we choose $\varepsilon_1 = 0.1/(\alpha^2 M^2)$. For HB and CHB, we choose $\beta = 0.4$. The values of the regularization parameter for logistic regression and lasso regression are $\lambda = 0.001$ and $\lambda = 0.1$, respectively. All regression tasks stop when the

objective error is less than 10^{-7} . Furthermore, we consider training a neural network with *Adult fat* dataset where we choose $\alpha = 0.01$ for all algorithms. For CHB and censoring-based GD, we choose $\varepsilon_1 = 0.01$. Again, for HB and CHB, we choose $\beta = 0.4$. The regularization parameter we choose for the neural network is $\lambda = 1/1605$. The optimization process is stopped after 500 iterations for training the neural network. Figure 6 and Figure 7 indicate the effectiveness of CHB in terms of communication reduction for the four learning tasks considered in this paper. The specific results are summarized in Table II.

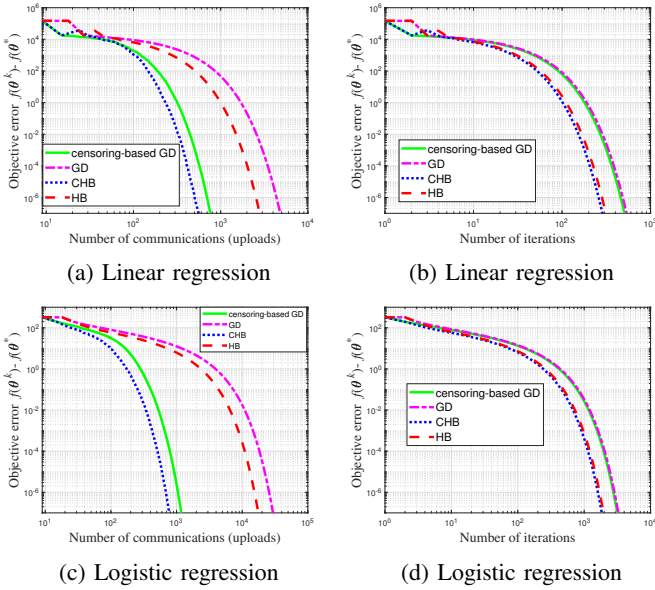


Fig. 6: Objective error for linear regression and logistic regression in the *Housing*, *Body fat*, *Abalone*, *Ionosphere*, *Adult fat*, and *Derm* datasets.

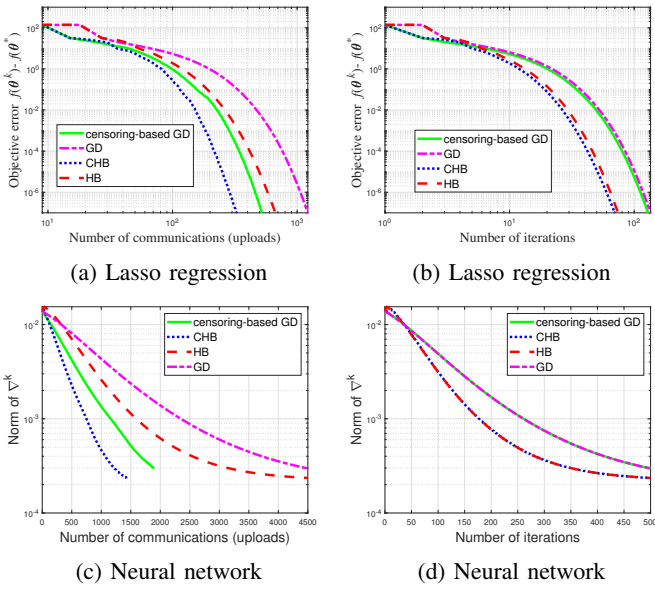


Fig. 7: Objective error for lasso regression and training a neural network in the *Ionosphere*, *Adult fat*, and *Derm* datasets.

We next test the performance of CHB on a larger dataset *MNIST* [63]. In all regression tasks, we set $\varepsilon_1 = 0.1/(\alpha^2 M^2)$ for CHB and censoring-based GD. For HB and CHB, we set $\beta = 0.4$. The largest number of iterations for each algorithm in each regression task is fixed to be 2000. For linear regression and lasso regression, we set $\alpha = 10^{-8}$. For logistic regression, we use $\alpha = 10^{-6}$. The values of regularization parameter for lasso regression and logistic regression are $\lambda = 0.5$ and $\lambda = 0.001$, respectively. In training a neural network with the regularization parameter $\lambda = 1/60000$, we choose $\alpha = 0.02$ for all algorithms. For CHB and censoring-based GD, we choose $\varepsilon_1 = 0.01$. For HB and CHB, we choose the constant $\beta = 0.4$. The largest number of iterations is set to be 500 in training a neural network. In Figure 8 and Figure 9, for the fixed total number of iterations, CHB shows a competitive communication saving performance while maintaining a relatively smaller objective error compared to GD and censoring-based GD. Specific results are summarized in Table III.

Furthermore, with the same parameter setting in the linear regression task on the MNIST dataset except for the step size, we consider the impact of the step size α on the number of communications needed to attain a target objective error. Figure 10(a) and Figure 10(b) indicates that choosing a large step size might speed up the optimization process (compare $\alpha = 2.2 \times 10^{-7}$ and $\alpha = 2.2 \times 10^{-8}$ at iteration 2000 which corresponds to the end point of each curve), but choosing a large step size might not save the largest number of communications for CHB and censoring-based GD, e.g., to attain the fixed objective error $\approx 10^4$, the number of communications of censoring-based GD for $\alpha = 2.2 \times 10^{-7}$ is 303 which is larger than that for $\alpha = 2.2 \times 10^{-8}$ with its number of communications being 205. Note that to attain the objective error $\approx 10^4$, even through censoring-based GD can save more communications than CHB for the case when $\alpha = 2.2 \times 10^{-7}$, this step size is not a good choice in term of communication savings. It is clear that censoring-based GD can save more communications if we choose $\alpha = 2.2 \times 10^{-8}$ and in this case CHB still outperforms censoring-based GD. In order to reduce the total number of communications, a relatively small step size is preferable for CHB and censoring-based GD. This illustrates the basic trade-off between the number of iterations and the number of communication in some cases, which is interesting. Communications can be saved using a relatively small step size which results in more iterations to attain a target accuracy. Additionally, Figure 10(d) illustrates that compared to GD and censoring-based GD, the momentum term can help CHB converge for a relatively large step size case.

Now we consider the impact of ε_1 on the communication savings and convergence of CHB. Specifically, with the same setting as Figure 3 except ε_1 , Figure 11 indicates that CHB with $\varepsilon_1 = 0.01/(\alpha^2 M^2)$ performs similarly to the classical HB in terms of the number of iterations while saving some communications for a given objective error. This is reasonable since smaller ε_1 indicates less communication censoring. When we increase ε_1 to $0.1/(\alpha^2 M^2)$, we can save more communications without too much impact on convergence. However, when ε_1 is too large, e.g., $\varepsilon_1 = 1/(\alpha^2 M^2)$, increased communication censoring will occur such that more iterations

TABLE II: Performance comparison in the *Ionosphere*, *Adult*, and *Derm* dataset. The objective error is 10^{-7} for all linear regression tasks. The fixed number of iterations for training the neural network is 500.

Name	Linear regression		Lasso regression		Logistic regression		Neural network	
	Comm.	Iter.	Comm.	Iter.	Comm.	Iter.	Comm.	Norm square grad.
CHB	559	287	329	70	772	1842	1436	2.3566×10^{-4}
HB	2808	312	675	75	17595	1955	4500	2.3547×10^{-4}
LAG	762	507	522	130	1179	3152	1899	2.9703×10^{-4}
GD	4824	536	1224	136	29439	3271	4500	2.9752×10^{-4}

are required to attain a given objective error. Figure 11 also indicates that CHB is able to achieve a good communication-iteration trade-off by tuning ε_1 .

From the previous numerical results where we plot the objective error versus the number of iterations for CHB and censoring-based GD, e.g., Figure 3, we can see that CHB provides faster convergence in these cases compared to censoring-based GD due to the momentum term in the update rule. The averaged per-communication descent is defined by $(f(\theta^0) - f(\theta^k)) / (\text{the total number of communications})$. Figure 12 shows that CHB has a larger averaged per-communication descent than censoring-based GD for a given objective error in this case. The results in Figure 12 also indicate that as the objective error becomes smaller (iteration k becomes larger), the averaged per-communication descent for both CHB and censoring-based GD becomes smaller for both algorithms. This is reasonable since the descent typically becomes smaller for larger k for both algorithms.

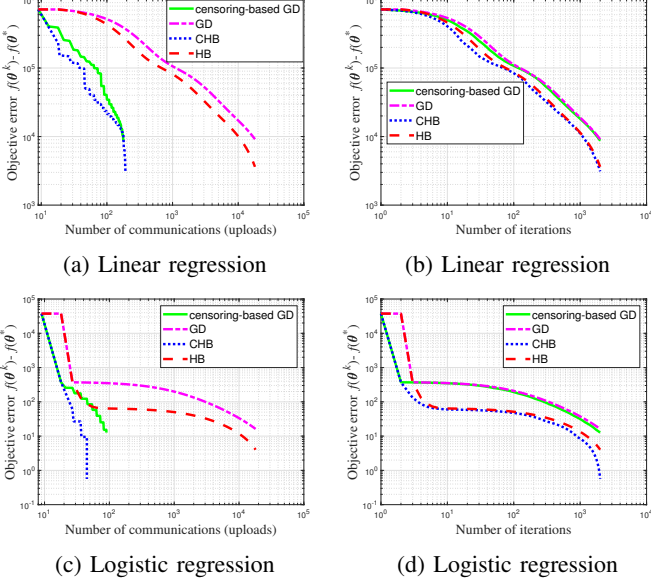


Fig. 8: Objective error for linear regression and logistic regression in the *MNIST* dataset.

V. CONCLUSION

This paper proposed a censoring-based heavy ball (CHB) method to optimize an objective function which is a sum of local functions in a communication-efficient manner. The key to save communications is to employ a censoring strategy

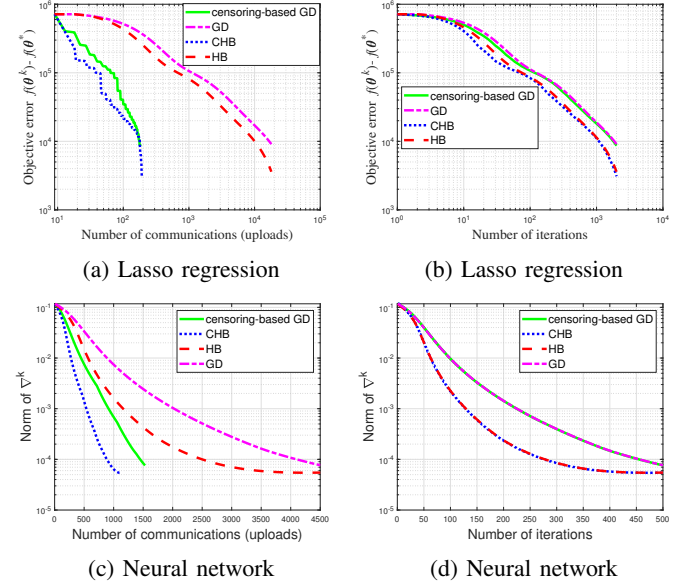


Fig. 9: Objective error for lasso regression and training a neural network in the *MNIST* dataset.

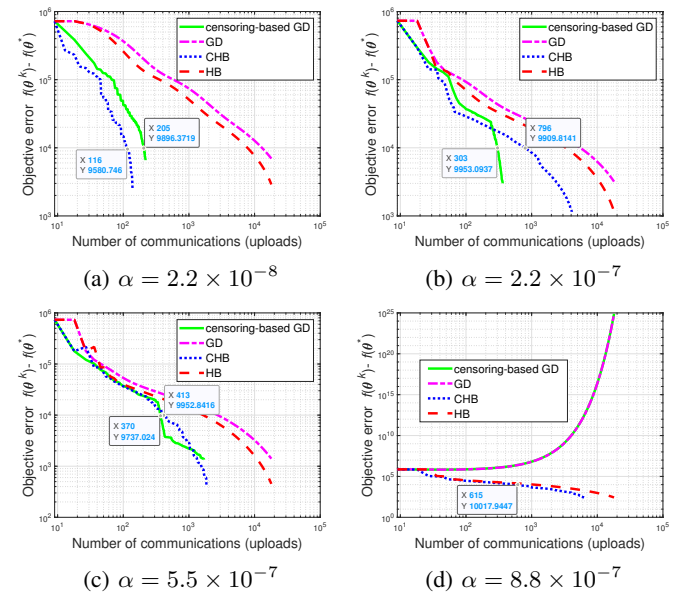


Fig. 10: Objective error for linear regression with different step sizes in the *MNIST* dataset.

where a worker is not allowed to transmit if its gradient is not sufficiently different from its previously transmitted

TABLE III: Performance comparison in the *MNIST* dataset at the accomplishment of the largest number of iterations.

Name	Linear regression			Lasso regression			Logistic regression		Neural network		
	Comm.	Obj. error		Comm.	Obj. error		Comm.	Obj. error	Comm.	Norm square grad.	
CHB	191	3.1077×10^3		191	3.0901×10^3		45	0.5621	1123	5.4545×10^{-5}	
HB	18000	3.6170×10^3		18000	3.5995×10^3		18000	4.0102	4500	5.4850×10^{-5}	
LAG	179	8.6826×10^3		184	8.6483×10^3		90	12.6540	1532	7.5920×10^{-5}	
GD	18000	9.1365×10^3		18000	9.1007×10^3		18000	16.1719	4500	7.6681×10^{-5}	

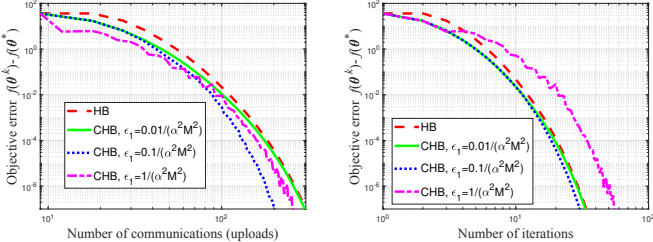
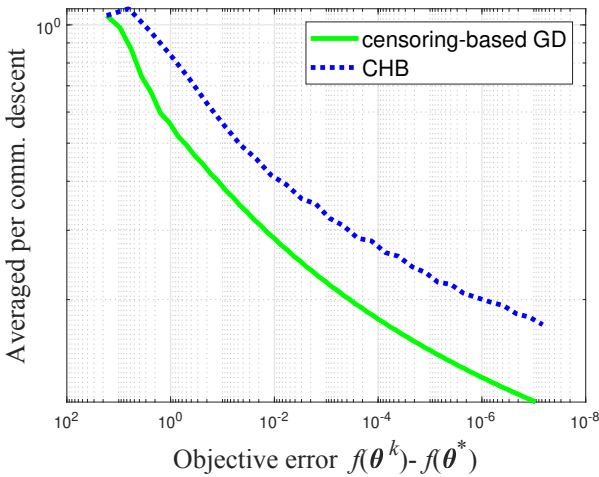
Fig. 11: Objective error versus the number of communications and iterations for logistic regression with different ϵ_1 in synthetic datasets.

Fig. 12: The averaged per-communication descent versus objective error for logistic regression with exactly the same setting as Figure 3.

one. The HB method provides smoothing and so it is well matched with gradient censoring. Compared to the classical HB method, CHB is able to significantly reduce the number of communications while maintaining a fast convergence rate for strongly convex, convex, and nonconvex objective functions. As we have shown, CHB can provide significant communications savings with very little impact on convergence rate, and CHB can also be tuned to trade-off communications and convergence rate if desired. In all cases numerical results validate the communication efficiency of CHB on both synthetic and real datasets. The CHB approach provides a new tool for reducing communications, and so it can potentially be applied along with other complementary techniques such as quantization, compression, and gradient sparsification, to make CHB more efficient in terms of bandwidth per communication as well

as the number of communications. Additionally, finding an optimal approach to tune the parameters of CHB, e.g., ϵ_1 , is also very interesting. Finally, we note that worker privacy and security are important considerations, and this should be combined with CHB.

APPENDIX A PROOF OF A USEFUL LEMMA

Lemma 3. Suppose $f(\theta)$ is L -smooth and let θ^{k+1} be generated by (4), then the CHB algorithm yields the following descent

$$f(\theta^{k+1}) - f(\theta^k) \leq -\frac{\alpha}{2} \|\nabla f(\theta^k)\|^2 - \frac{1-\alpha L}{2\alpha} \|\theta^{k+1} - \theta^k\|^2 + \left\| \sqrt{\frac{\alpha}{2}} \sum_{m \in \mathcal{M}_c^k} \delta \nabla_m^k + \frac{\beta}{\sqrt{2\alpha}} (\theta^k - \theta^{k-1}) \right\|^2. \quad (22)$$

Proof: From Assumption 1 we know [58]

$$f(\theta^{k+1}) - f(\theta^k) \leq \langle \nabla f(\theta^k), \theta^{k+1} - \theta^k \rangle + \frac{L}{2} \|\theta^{k+1} - \theta^k\|^2. \quad (23)$$

Using (6) in $\langle \nabla f(\theta^k), \theta^{k+1} - \theta^k \rangle$ yields

$$\begin{aligned} & \langle \nabla f(\theta^k), \theta^{k+1} - \theta^k \rangle \\ &= -\alpha \langle \nabla f(\theta^k), \nabla f(\theta^k) - \sum_{m \in \mathcal{M}_c^k} \delta \nabla_m^k \rangle \\ & \quad + \beta \langle \nabla f(\theta^k), \theta^k - \theta^{k-1} \rangle \end{aligned} \quad (24)$$

$$\begin{aligned} &= -\alpha \|\nabla f(\theta^k)\|^2 + \left\langle \sqrt{\alpha} \nabla f(\theta^k), \sqrt{\alpha} \sum_{m \in \mathcal{M}_c^k} \delta \nabla_m^k \right\rangle \\ & \quad + \beta \langle \nabla f(\theta^k), \theta^k - \theta^{k-1} \rangle \\ &= -\alpha \|\nabla f(\theta^k)\|^2 + \frac{\alpha}{2} \|\nabla f(\theta^k)\|^2 + \frac{\alpha}{2} \left\| \sum_{m \in \mathcal{M}_c^k} \delta \nabla_m^k \right\|^2 \\ & \quad - \frac{\alpha}{2} \left\| \nabla f(\theta^k) - \sum_{m \in \mathcal{M}_c^k} \delta \nabla_m^k \right\|^2 + \beta \langle \nabla f(\theta^k), \theta^k - \theta^{k-1} \rangle. \end{aligned} \quad (25)$$

To go from (25) to (26), the quality $\langle \mathbf{x}, \mathbf{y} \rangle = \frac{1}{2} \|\mathbf{x}\|^2 + \frac{1}{2} \|\mathbf{y}\|^2 - \frac{1}{2} \|\mathbf{x} - \mathbf{y}\|^2$ is employed for the term $\langle \sqrt{\alpha} \nabla f(\theta^k), \sqrt{\alpha} \sum_{m \in \mathcal{M}_c^k} \delta \nabla_m^k \rangle$.

From (6), we obtain that

$$\begin{aligned} & \|\theta^{k+1} - \theta^k\|^2 \\ &= \alpha^2 \left\| \nabla f(\theta^k) - \sum_{m \in \mathcal{M}_c^k} \delta \nabla_m^k \right\|^2 + \beta^2 \|\theta^k - \theta^{k-1}\|^2 \\ & \quad - 2\alpha\beta \langle \nabla f(\theta^k), \theta^k - \theta^{k-1} \rangle \end{aligned}$$

$$+ 2\alpha\beta \left\langle \sum_{m \in \mathcal{M}_c^k} \delta \nabla_m^k, \boldsymbol{\theta}^k - \boldsymbol{\theta}^{k-1} \right\rangle. \quad (27)$$

Plugging (26) and (27) into (23), we obtain

$$\begin{aligned} & f(\boldsymbol{\theta}^{k+1}) - f(\boldsymbol{\theta}^k) \\ & \leq -\frac{\alpha}{2} \|\nabla f(\boldsymbol{\theta}^k)\|^2 - \frac{\alpha(1-\alpha L)}{2} \left\| \nabla f(\boldsymbol{\theta}^k) - \sum_{m \in \mathcal{M}_c^k} \delta \nabla_m^k \right\|^2 \\ & \quad + \frac{\alpha}{2} \left\| \sum_{m \in \mathcal{M}_c^k} \delta \nabla_m^k \right\|^2 + \frac{L\beta^2}{2} \|\boldsymbol{\theta}^k - \boldsymbol{\theta}^{k-1}\|^2 \\ & \quad + \beta(1-\alpha L) \left\langle \nabla f(\boldsymbol{\theta}^k), \boldsymbol{\theta}^k - \boldsymbol{\theta}^{k-1} \right\rangle \\ & \quad + \alpha\beta L \left\langle \sum_{m \in \mathcal{M}_c^k} \delta \nabla_m^k, \boldsymbol{\theta}^k - \boldsymbol{\theta}^{k-1} \right\rangle. \end{aligned} \quad (28)$$

Multiplying both sides of (27) by a constant $(1-\alpha L)/(2\alpha)$ implies

$$\begin{aligned} & \frac{1-\alpha L}{2\alpha} \|\boldsymbol{\theta}^{k+1} - \boldsymbol{\theta}^k\|^2 \\ & = \frac{\alpha(1-\alpha L)}{2} \left\| \nabla f(\boldsymbol{\theta}^k) - \sum_{m \in \mathcal{M}_c^k} \delta \nabla_m^k \right\|^2 \\ & \quad + \frac{(1-\alpha L)\beta^2}{2\alpha} \|\boldsymbol{\theta}^k - \boldsymbol{\theta}^{k-1}\|^2 \\ & \quad - \beta(1-\alpha L) \left\langle \nabla f(\boldsymbol{\theta}^k), \boldsymbol{\theta}^k - \boldsymbol{\theta}^{k-1} \right\rangle \\ & \quad + (1-\alpha L)\beta \left\langle \sum_{m \in \mathcal{M}_c^k} \delta \nabla_m^k, \boldsymbol{\theta}^k - \boldsymbol{\theta}^{k-1} \right\rangle. \end{aligned} \quad (29)$$

Adding (29) to (28) yields

$$\begin{aligned} & f(\boldsymbol{\theta}^{k+1}) + \frac{1-\alpha L}{2\alpha} \|\boldsymbol{\theta}^{k+1} - \boldsymbol{\theta}^k\|^2 \\ & \leq f(\boldsymbol{\theta}^k) - \frac{\alpha}{2} \|\nabla f(\boldsymbol{\theta}^k)\|^2 + \frac{\beta^2}{2\alpha} \|\boldsymbol{\theta}^k - \boldsymbol{\theta}^{k-1}\|^2 \\ & \quad + \frac{\alpha}{2} \left\| \sum_{m \in \mathcal{M}_c^k} \delta \nabla_m^k \right\|^2 + \beta \left\langle \sum_{m \in \mathcal{M}_c^k} \delta \nabla_m^k, \boldsymbol{\theta}^k - \boldsymbol{\theta}^{k-1} \right\rangle \end{aligned} \quad (30)$$

$$\begin{aligned} & \leq f(\boldsymbol{\theta}^k) - \frac{\alpha}{2} \|\nabla f(\boldsymbol{\theta}^k)\|^2 \\ & \quad + \left\| \sqrt{\frac{\alpha}{2}} \sum_{m \in \mathcal{M}_c^k} \delta \nabla_m^k + \frac{\beta}{\sqrt{2\alpha}} (\boldsymbol{\theta}^k - \boldsymbol{\theta}^{k-1}) \right\|^2. \end{aligned} \quad (31)$$

The result in (22) follows after rearranging terms in (31). ■

APPENDIX B PROOF OF LEMMA 1

With $\mathbb{L}(\boldsymbol{\theta}^k)$ in (9), it can be shown that

$$\begin{aligned} & \mathbb{L}(\boldsymbol{\theta}^{k+1}) - \mathbb{L}(\boldsymbol{\theta}^k) \\ & = f(\boldsymbol{\theta}^{k+1}) - f(\boldsymbol{\theta}^k) + \eta_1 \|\boldsymbol{\theta}^{k+1} - \boldsymbol{\theta}^k\|^2 - \eta_1 \|\boldsymbol{\theta}^k - \boldsymbol{\theta}^{k-1}\|^2. \end{aligned} \quad (32)$$

Plugging (22) into (32) yields

$$\begin{aligned} & \mathbb{L}(\boldsymbol{\theta}^{k+1}) - \mathbb{L}(\boldsymbol{\theta}^k) \\ & \leq -\frac{\alpha}{2} \|\nabla f(\boldsymbol{\theta}^k)\|^2 + \left(\eta_1 - \frac{1-\alpha L}{2\alpha} \right) \|\boldsymbol{\theta}^{k+1} - \boldsymbol{\theta}^k\|^2 \end{aligned}$$

$$\begin{aligned} & + \left\| \sqrt{\frac{\alpha}{2}} \sum_{m \in \mathcal{M}_c^k} \delta \nabla_m^k + \frac{\beta}{\sqrt{2\alpha}} (\boldsymbol{\theta}^k - \boldsymbol{\theta}^{k-1}) \right\|^2 \\ & - \eta_1 \|\boldsymbol{\theta}^k - \boldsymbol{\theta}^{k-1}\|^2 \end{aligned} \quad (33)$$

$$\begin{aligned} & \leq -\frac{\alpha}{2} \|\nabla f(\boldsymbol{\theta}^k)\|^2 + \left(\eta_1 - \frac{1-\alpha L}{2\alpha} \right) \|\boldsymbol{\theta}^{k+1} - \boldsymbol{\theta}^k\|^2 \\ & \quad + \frac{\alpha}{2} (1+\rho_3) \left\| \sum_{m \in \mathcal{M}_c^k} \delta \nabla_m^k \right\|^2 \\ & \quad + \frac{\beta^2}{2\alpha} (1+\rho_3^{-1}) \|\boldsymbol{\theta}^k - \boldsymbol{\theta}^{k-1}\|^2 - \eta_1 \|\boldsymbol{\theta}^k - \boldsymbol{\theta}^{k-1}\|^2 \end{aligned} \quad (34)$$

where ρ_3 is any positive number. In going from (33) to (34), we employ Young's inequality: $\|\mathbf{x} + \mathbf{y}\|^2 \leq (1+\rho)\|\mathbf{x}\|^2 + (1+\rho^{-1})\|\mathbf{y}\|^2, \forall \rho > 0$. From (6), we have

$$\begin{aligned} & \|\boldsymbol{\theta}^{k+1} - \boldsymbol{\theta}^k\|^2 \\ & = \left\| -\alpha \left(\nabla f(\boldsymbol{\theta}^k) - \sum_{m \in \mathcal{M}_c^k} \delta \nabla_m^k \right) + \beta (\boldsymbol{\theta}^k - \boldsymbol{\theta}^{k-1}) \right\|^2 \end{aligned} \quad (35)$$

$$\begin{aligned} & \leq \alpha^2 (1+\rho_1) \left((1+\rho_2) \left\| \nabla f(\boldsymbol{\theta}^k) \right\|^2 \right. \\ & \quad \left. + (1+\rho_2^{-1}) \left\| \sum_{m \in \mathcal{M}_c^k} \delta \nabla_m^k \right\|^2 \right) \\ & \quad + \beta^2 (1+\rho_1^{-1}) \|\boldsymbol{\theta}^k - \boldsymbol{\theta}^{k-1}\|^2 \end{aligned} \quad (36)$$

where ρ_1 and ρ_2 are any positive numbers, and the inequality in (36) is obtained using Young's inequality. Using (36) in (34) along with $\eta_1 - \frac{1-\alpha L}{2\alpha} \geq 0$, yields

$$\begin{aligned} & \mathbb{L}(\boldsymbol{\theta}^{k+1}) - \mathbb{L}(\boldsymbol{\theta}^k) \\ & \leq \left(-\frac{\alpha}{2} + \left(\eta_1 - \frac{1-\alpha L}{2\alpha} \right) \alpha^2 (1+\rho_1)(1+\rho_2) \right) \|\nabla f(\boldsymbol{\theta}^k)\|^2 \\ & \quad + \left(\left(\eta_1 - \frac{1-\alpha L}{2\alpha} \right) \alpha^2 (1+\rho_1)(1+\rho_2^{-1}) \right. \\ & \quad \left. + \frac{\alpha}{2} (1+\rho_3) \right) \left\| \sum_{m \in \mathcal{M}_c^k} \delta \nabla_m^k \right\|^2 \\ & \quad + \left(\frac{\beta^2}{2\alpha} (1+\rho_3^{-1}) - \eta_1 \right. \\ & \quad \left. + \left(\eta_1 - \frac{1-\alpha L}{2\alpha} \right) \beta^2 (1+\rho_1^{-1}) \right) \|\boldsymbol{\theta}^k - \boldsymbol{\theta}^{k-1}\|^2. \end{aligned} \quad (37)$$

Employing the inequality $\left\| \sum_{n=1}^N \mathbf{x}_n \right\|^2 \leq N \sum_{n=1}^N \|\mathbf{x}_n\|^2$, $\left\| \sum_{m \in \mathcal{M}_c^k} \delta \nabla_m^k \right\|^2$ can be bounded by

$$\begin{aligned} & \left\| \sum_{m \in \mathcal{M}_c^k} \delta \nabla_m^k \right\|^2 \leq |\mathcal{M}_c^k| \sum_{m \in \mathcal{M}_c^k} \left\| \delta \nabla_m^k \right\|^2 \\ & \leq |\mathcal{M}_c^k|^2 \varepsilon_1 \|\boldsymbol{\theta}^k - \boldsymbol{\theta}^{k-1}\|^2 \end{aligned} \quad (38)$$

where (38) is obtained using the CHB-skip-transmission condition in (8).

Plugging (38) into (37) with $\gamma \triangleq \frac{\alpha}{2}(1 + \rho_3) + \left(\eta_1 - \frac{1-\alpha L}{2\alpha}\right)\alpha^2(1 + \rho_1)(1 + \rho_2^{-1})$ and $\eta_1 - \frac{1-\alpha L}{2\alpha} \geq 0$, we obtain

$$\begin{aligned} & \mathbb{L}(\boldsymbol{\theta}^{k+1}) - \mathbb{L}(\boldsymbol{\theta}^k) \\ & \leq \left(-\frac{\alpha}{2} + \left(\eta_1 - \frac{1-\alpha L}{2\alpha}\right)\alpha^2(1 + \rho_1)(1 + \rho_2) \right) \|\nabla f(\boldsymbol{\theta}^k)\|^2 \\ & \quad + \left(\left(\eta_1 - \frac{1-\alpha L}{2\alpha}\right)\beta^2(1 + \rho_1^{-1}) + |\mathcal{M}_c^k|^2\varepsilon_1\gamma \right. \\ & \quad \left. + \frac{\beta^2}{2\alpha}(1 + \rho_3^{-1}) - \eta_1 \right) \|\boldsymbol{\theta}^k - \boldsymbol{\theta}^{k-1}\|^2. \end{aligned} \quad (39)$$

Note that $\eta_1 - \frac{1-\alpha L}{2\alpha} \geq 0$ implies $\gamma \geq \frac{\alpha}{2}(1 + \rho_3) > 0$. The proof is complete after defining the non-negative constants σ_0 and σ_1 as shown in (10) and (11), respectively. Since the expressions of σ_0 and σ_1 are complicated, we provide several choices of parameters in the following.

a) *Parameter Choices:* First note that (10)–(12) are equivalent to

$$\frac{1}{2\eta_1 + L} \leq \alpha \leq \frac{1 + (1 + \rho_1)(1 + \rho_2)}{(2\eta_1 + L)(1 + \rho_1)(1 + \rho_2)}, \quad (40)$$

$$\beta \leq \sqrt{\frac{2\alpha\eta_1}{(1 + \rho_3^{-1}) + (1 + \rho_1^{-1})(2\alpha\eta_1 - 1 + \alpha L)}}, \quad (41)$$

$$\varepsilon_1 \leq \frac{\eta_1 - \beta^2\left(\frac{1+\rho_3^{-1}}{2\alpha} + (\eta_1 - \frac{1-\alpha L}{2\alpha})(1 + \rho_1^{-1})\right)}{|\mathcal{M}_c^k|^2\gamma}. \quad (42)$$

• Setting $\eta_1 = \frac{1-\alpha L}{2\alpha}$, (40)–(42) are equivalent to

$$\alpha \leq \frac{1}{L}, \quad \beta \leq \sqrt{\frac{1 - \alpha L}{1 + \rho_3^{-1}}}, \quad \varepsilon_1 \leq \frac{(1 - \alpha L) - \beta^2(1 + \rho_3^{-1})}{\alpha^2(1 + \rho_3)|\mathcal{M}_c^k|^2}. \quad (43)$$

• Imposing $\eta_1 = 0$, $\rho_1 = 0$, and $\rho_2 = 0$ shows that (40)–(42) degenerate to $1/L \leq \alpha \leq 2/L$, $\beta = 0$, and $\varepsilon_1 = 0$.

• For $\alpha = 1/L$ and $\eta_1 > 0$, we find (40)–(42) are equivalent to

$$\begin{aligned} 0 \leq \eta_1 & \leq \frac{L}{2(1 + \rho_1)(1 + \rho_2)}, \\ \beta^2 & \leq \frac{2\eta_1}{2\eta_1(1 + \rho_1^{-1}) + L(1 + \rho_3^{-1})}, \\ \varepsilon_1 & \leq \frac{L^2\left(2\eta_1 - \beta^2(L(1 + \rho_3^{-1}) + 2\eta_1(1 + \rho_1^{-1}))\right)}{|\mathcal{M}_c^k|^2\left(L(1 + \rho_3) + 2\eta_1(1 + \rho_1)(1 + \rho_2^{-1})\right)}. \end{aligned} \quad (44)$$

APPENDIX C PROOF OF THEOREM 1

From strong convexity from Definition 1, $f(\boldsymbol{\theta})$ satisfies [58]

$$2\mu(f(\boldsymbol{\theta}^k) - f(\boldsymbol{\theta}^*)) \leq \|\nabla f(\boldsymbol{\theta}^k)\|^2 \quad (45)$$

where $\boldsymbol{\theta}^*$ denotes the minimizer of (1). Using (45) in (39) with $\sigma_0 \geq 0$ in (10) and $\eta_1 \neq 0$ yields

$$\mathbb{L}(\boldsymbol{\theta}^{k+1}) - \mathbb{L}(\boldsymbol{\theta}^k)$$

$$\begin{aligned} & \leq \left(2\mu\left(\eta_1 - \frac{1-\alpha L}{2\alpha}\right)\alpha^2(1 + \rho_1)(1 + \rho_2) \right. \\ & \quad \left. - \alpha\mu \right) (f(\boldsymbol{\theta}^k) - f(\boldsymbol{\theta}^*)) \\ & \quad + \left(\frac{\beta^2}{2\alpha}(1 + \rho_3^{-1}) - \eta_1 + \left(\eta_1 - \frac{1-\alpha L}{2\alpha}\right)\beta^2(1 + \rho_1^{-1}) \right. \\ & \quad \left. + |\mathcal{M}_c^k|^2\varepsilon_1\gamma \right) \|\boldsymbol{\theta}^k - \boldsymbol{\theta}^{k-1}\|^2 \end{aligned} \quad (46)$$

$$\begin{aligned} & = - \left(-\left(2\eta_1 - \frac{1-\alpha L}{\alpha}\right)\alpha^2\mu(1 + \rho_1)(1 + \rho_2) \right. \\ & \quad \left. + \alpha\mu \right) (f(\boldsymbol{\theta}^k) - f(\boldsymbol{\theta}^*)) \\ & \quad - \left(1 - \frac{\beta^2}{2\alpha\eta_1}(1 + \rho_3^{-1}) - \left(1 - \frac{1-\alpha L}{2\alpha\eta_1}\right)\beta^2(1 + \rho_1^{-1}) \right. \\ & \quad \left. - \frac{|\mathcal{M}_c^k|^2\varepsilon_1\gamma}{\eta_1} \right) \eta_1 \|\boldsymbol{\theta}^k - \boldsymbol{\theta}^{k-1}\|^2 \end{aligned} \quad (47)$$

Define

$$\begin{aligned} & c(\alpha, \beta, \varepsilon_1) \\ & \triangleq \min \left\{ \alpha\mu - \left(2\eta_1 - \frac{1-\alpha L}{\alpha}\right)\alpha^2\mu(1 + \rho_1)(1 + \rho_2), \right. \\ & \quad \left. \min_k \left\{ 1 - \frac{\beta^2}{2\alpha\eta_1}(1 + \rho_3^{-1}) - \left(1 - \frac{1-\alpha L}{2\alpha\eta_1}\right)\beta^2(1 + \rho_1^{-1}) \right. \right. \\ & \quad \left. \left. - \frac{|\mathcal{M}_c^k|^2\varepsilon_1\gamma}{\eta_1} \right\} \right\} \end{aligned} \quad (48)$$

$$= \min \left\{ 2\sigma_0\mu, \min_k \{\sigma_1\} / \eta_1 \right\}. \quad (49)$$

The result in (49) follows from the expressions for σ_0 and σ_1 in (10) and (11), respectively. Using (47) and (48) yields

$$\begin{aligned} & \mathbb{L}(\boldsymbol{\theta}^{k+1}) - \mathbb{L}(\boldsymbol{\theta}^k) \\ & \leq -c(\alpha, \beta, \varepsilon_1) \left(f(\boldsymbol{\theta}^k) - f(\boldsymbol{\theta}^*) + \eta_1 \|\boldsymbol{\theta}^k - \boldsymbol{\theta}^{k-1}\|^2 \right) \end{aligned} \quad (50)$$

$$= -c(\alpha, \beta, \varepsilon_1) \mathbb{L}(\boldsymbol{\theta}^k) \quad (51)$$

which implies

$$\mathbb{L}(\boldsymbol{\theta}^{k+1}) \leq (1 - c(\alpha, \beta, \varepsilon_1)) \mathbb{L}(\boldsymbol{\theta}^k). \quad (52)$$

It is clear that when (10)–(11) are satisfied with $\sigma_0 > 0$ in (10) and $\sigma_1 > 0$ in (11), we have $c(\alpha, \beta, \varepsilon_1) > 0$. If (12) is satisfied, then we can obtain $c(\alpha, \beta, \varepsilon_1) < 1$ from (48). Thus, we have $c(\alpha, \beta, \varepsilon_1) \in (0, 1)$. The result in (52) indicates the Q-linear convergence of $\mathbb{L}(\boldsymbol{\theta}^k)$. Since η_1 is non-negative in the definition of $\mathbb{L}(\boldsymbol{\theta}^k)$, the result in (52) implies that

$$f(\boldsymbol{\theta}^k) - f(\boldsymbol{\theta}^*) \leq (1 - c(\alpha, \beta, \varepsilon_1))^k \mathbb{L}(\boldsymbol{\theta}^0), \quad (53)$$

which completes the proof. Consider a case with $\eta_1 - \frac{1-\alpha L}{2\alpha} = 0$ with $\eta_1 \neq 0$. Then (12) yields $\gamma = \alpha(1 + \rho_3)/2$, and (48) yields

$$c(\alpha, \beta, \varepsilon_1)$$

$$= \min_k \left\{ \alpha\mu, 1 - \frac{\beta^2}{1-\alpha L}(1+\rho_3^{-1}) - \frac{\alpha^2(1+\rho_3)|\mathcal{M}_c^k|^2\varepsilon_1}{1-\alpha L} \right\}. \quad (54)$$

Setting $\rho_3 = 1$, $\delta \in (0, 1)$, and $\alpha = \frac{1-\delta}{L}$, gives

$$\eta_1 = \frac{1-\alpha L}{2\alpha}, \varepsilon_1 = \frac{(1-\alpha L)(1-\alpha\mu)}{4\alpha^2 M^2},$$

$$\text{and } \beta = \frac{1}{2}\sqrt{(1-\alpha L)(1-\alpha\mu)}, \quad (55)$$

and (54) yields

$$c(\alpha, \beta, \varepsilon_1) = \min_k \left\{ \alpha\mu, 1 - \frac{1-\alpha\mu}{2} \left(1 + \frac{|\mathcal{M}_c^k|^2}{M^2} \right) \right\}$$

$$= \alpha\mu. \quad (56)$$

It follows that

$$\frac{\mathbb{L}(\boldsymbol{\theta}^{k+1})}{\mathbb{L}(\boldsymbol{\theta}^1)} \leq \left(1 - \frac{1-\delta}{L/\mu} \right)^k \leq \epsilon. \quad (57)$$

Rearranging terms in (57), yields

$$\log\left(\frac{1}{\epsilon}\right) \leq k \log\left(1 + \frac{1}{\frac{L/\mu}{1-\delta} - 1}\right) \leq \frac{k}{\frac{L/\mu}{1-\delta} - 1} \quad (58)$$

such that the iteration complexity $\mathbb{I}_{CHB}(\epsilon)$ is

$$\mathbb{I}_{CHB}(\epsilon) = \frac{L/\mu}{1-\delta} \log\left(\frac{1}{\epsilon}\right). \quad (59)$$

APPENDIX D PROOF OF THEOREM 2

The following is inspired by the previous work in [54] which can be regarded as a special case of CHB without the momentum term (with $\beta = 0$). We start with a lemma that will be helpful later.

Lemma 4. *Under Definition 2, the Lyapunov function $\mathbb{L}(\boldsymbol{\theta}^k)$ satisfies*

$$\mathbb{L}(\boldsymbol{\theta}^k) \leq \sqrt{\left(\|\nabla f(\boldsymbol{\theta}^k)\|^2 + \eta_1 \|\boldsymbol{\theta}^k - \boldsymbol{\theta}^{k-1}\|^2 \right)} \cdot \sqrt{\left(\|\boldsymbol{\theta}^k - \boldsymbol{\theta}^*\|^2 + \eta_1 \|\boldsymbol{\theta}^k - \boldsymbol{\theta}^{k-1}\|^2 \right)}. \quad (60)$$

Proof: Using Definition 2 (convexity)

$$f(\boldsymbol{\theta}^k) - f(\boldsymbol{\theta}^*) \leq \langle \nabla f(\boldsymbol{\theta}^k), \boldsymbol{\theta}^k - \boldsymbol{\theta}^* \rangle. \quad (61)$$

Thus

$$\begin{aligned} \mathbb{L}(\boldsymbol{\theta}^k) &= f(\boldsymbol{\theta}^k) - f(\boldsymbol{\theta}^*) + \eta_1 \|\boldsymbol{\theta}^k - \boldsymbol{\theta}^{k-1}\|^2 \\ &\leq \langle \nabla f(\boldsymbol{\theta}^k), \boldsymbol{\theta}^k - \boldsymbol{\theta}^* \rangle \\ &\quad + \langle \sqrt{\eta_1} \|\boldsymbol{\theta}^k - \boldsymbol{\theta}^{k-1}\|, \sqrt{\eta_1} \|\boldsymbol{\theta}^k - \boldsymbol{\theta}^{k-1}\| \rangle \end{aligned} \quad (62)$$

$$= \left\langle \begin{bmatrix} \nabla f(\boldsymbol{\theta}^k), \sqrt{\eta_1} \|\boldsymbol{\theta}^k - \boldsymbol{\theta}^{k-1}\| \end{bmatrix}^\top, \begin{bmatrix} \boldsymbol{\theta}^k - \boldsymbol{\theta}^*, \sqrt{\eta_1} \|\boldsymbol{\theta}^k - \boldsymbol{\theta}^{k-1}\| \end{bmatrix}^\top \right\rangle \quad (63)$$

$$\leq \sqrt{\left(\|\nabla f(\boldsymbol{\theta}^k)\|^2 + \eta_1 \|\boldsymbol{\theta}^k - \boldsymbol{\theta}^{k-1}\|^2 \right)}$$

$$\cdot \sqrt{\left(\|\boldsymbol{\theta}^k - \boldsymbol{\theta}^*\|^2 + \eta_1 \|\boldsymbol{\theta}^k - \boldsymbol{\theta}^{k-1}\|^2 \right)}. \quad (64)$$

We obtained (62) by using (61). We use (63) and the inequality $\langle \mathbf{x}, \mathbf{y} \rangle \leq \|\mathbf{x}\| \|\mathbf{y}\|$ to obtain (64). This completes the proof. \blacksquare

Given Assumption 1 and assuming the constants α , β , and ε_1 satisfy (10)–(12) while $\sigma_0 > 0$ and $\sigma_1 > 0$, then (13) of Lemma 1 suggests that

$$\mathbb{L}(\boldsymbol{\theta}^{k+1}) - \mathbb{L}(\boldsymbol{\theta}^k) \leq -\sigma_0 \|\nabla f(\boldsymbol{\theta}^k)\|^2 - \sigma_1 \|\boldsymbol{\theta}^k - \boldsymbol{\theta}^{k-1}\|^2 \quad (65)$$

$$\leq -\min_k \{\sigma_0, \frac{\sigma_1}{\eta_1}\} \left(\|\nabla f(\boldsymbol{\theta}^k)\|^2 + \eta_1 \|\boldsymbol{\theta}^k - \boldsymbol{\theta}^{k-1}\|^2 \right). \quad (66)$$

Further, $\min_k \{\sigma_0, \frac{\sigma_1}{\eta_1}\} > 0$ with σ_0 and σ_1 provided in (10) and (11). Note that (66) yields

$$\begin{aligned} &\|\nabla f(\boldsymbol{\theta}^k)\|^2 + \eta_1 \|\boldsymbol{\theta}^k - \boldsymbol{\theta}^{k-1}\|^2 \\ &\leq \frac{1}{\min_k \{\sigma_0, \sigma_1/\eta_1\}} (\mathbb{L}(\boldsymbol{\theta}^k) - \mathbb{L}(\boldsymbol{\theta}^{k+1})). \end{aligned} \quad (67)$$

Assumption 1 implies that $\|\boldsymbol{\theta}^k - \boldsymbol{\theta}^*\| < +\infty$ and $\|\boldsymbol{\theta}^k - \boldsymbol{\theta}^{k-1}\| < +\infty$. It follows that

$$\|\boldsymbol{\theta}^k - \boldsymbol{\theta}^*\|^2 + \eta_1 \|\boldsymbol{\theta}^k - \boldsymbol{\theta}^{k-1}\|^2 \leq N. \quad (68)$$

for finite N . We can use (67) and (68) in (64) to show that

$$\begin{aligned} &(\mathbb{L}(\boldsymbol{\theta}^k))^2 \\ &\leq \left(\|\nabla f(\boldsymbol{\theta}^k)\|^2 + \eta_1 \|\boldsymbol{\theta}^k - \boldsymbol{\theta}^{k-1}\|^2 \right) \\ &\quad \left(\|\boldsymbol{\theta}^k - \boldsymbol{\theta}^*\|^2 + \eta_1 \|\boldsymbol{\theta}^k - \boldsymbol{\theta}^{k-1}\|^2 \right) \end{aligned} \quad (69)$$

$$\leq \frac{N}{\min_k \{\sigma_0, \sigma_1/\eta_1\}} (\mathbb{L}(\boldsymbol{\theta}^k) - \mathbb{L}(\boldsymbol{\theta}^{k+1})). \quad (70)$$

Lemma 1 implies that $\mathbb{L}(\boldsymbol{\theta}^k) \mathbb{L}(\boldsymbol{\theta}^{k+1}) \leq (\mathbb{L}(\boldsymbol{\theta}^k))^2$ so that (70) yields

$$\mathbb{L}(\boldsymbol{\theta}^k) \mathbb{L}(\boldsymbol{\theta}^{k+1}) \leq \frac{N}{\min_k \{\sigma_0, \sigma_1/\eta_1\}} (\mathbb{L}(\boldsymbol{\theta}^k) - \mathbb{L}(\boldsymbol{\theta}^{k+1})) \quad (71)$$

or

$$\frac{1}{\mathbb{L}(\boldsymbol{\theta}^{k+1})} - \frac{1}{\mathbb{L}(\boldsymbol{\theta}^k)} \geq \frac{\min_k \{\sigma_0, \sigma_1/\eta_1\}}{N}. \quad (72)$$

It follows that

$$\frac{1}{\mathbb{L}(\boldsymbol{\theta}^K)} \geq \frac{1}{\mathbb{L}(\boldsymbol{\theta}^K)} - \frac{1}{\mathbb{L}(\boldsymbol{\theta}^0)} \geq \frac{K \min_k \{\sigma_0, \sigma_1/\eta_1\}}{N}, \quad (73)$$

which completes the proof.

APPENDIX E PROOF OF THEOREM 3

This section again builds on [54]. From Lemma 1

$$\begin{aligned} \mathbb{L}(\boldsymbol{\theta}^{k+1}) - \mathbb{L}(\boldsymbol{\theta}^k) &\leq -\sigma_0 \|\nabla f(\boldsymbol{\theta}^k)\|^2 - \sigma_1 \|\boldsymbol{\theta}^k - \boldsymbol{\theta}^{k-1}\|^2 \\ &\leq -\min_k \{\sigma_0, \frac{\sigma_1}{\eta_1}\} \left(\|\nabla f(\boldsymbol{\theta}^k)\|^2 + \eta_1 \|\boldsymbol{\theta}^k - \boldsymbol{\theta}^{k-1}\|^2 \right). \end{aligned} \quad (74)$$

$$\leq -\min_k \{\sigma_0, \frac{\sigma_1}{\eta_1}\} \left(\|\nabla f(\boldsymbol{\theta}^k)\|^2 + \eta_1 \|\boldsymbol{\theta}^k - \boldsymbol{\theta}^{k-1}\|^2 \right). \quad (75)$$

The last equation is summed over k from 1 to K to yield

$$\begin{aligned} & \mathbb{L}(\boldsymbol{\theta}^1) - \mathbb{L}(\boldsymbol{\theta}^{K+1}) \\ & \geq \min_k \left\{ \sigma_0, \frac{\sigma_1}{\eta_1} \right\} \sum_{k=1}^K \left(\|\nabla f(\boldsymbol{\theta}^k)\|^2 + \eta_1 \|\boldsymbol{\theta}^k - \boldsymbol{\theta}^{k-1}\|^2 \right). \end{aligned} \quad (76)$$

Note that $\mathbb{L}(\boldsymbol{\theta}^1) - \mathbb{L}(\boldsymbol{\theta}^{K+1}) \leq \mathbb{L}(\boldsymbol{\theta}^1) < \infty$ so that

$$\lim_{K \rightarrow \infty} \sum_{k=1}^K \left(\|\nabla f(\boldsymbol{\theta}^k)\|^2 + \eta_1 \|\boldsymbol{\theta}^k - \boldsymbol{\theta}^{k-1}\|^2 \right) < \infty \quad (77)$$

or

$$\lim_{K \rightarrow \infty} \|\nabla f(\boldsymbol{\theta}^K)\|^2 \rightarrow 0. \quad (78)$$

APPENDIX F PROOF OF LEMMA 2

Suppose that worker m has communicated with the server at iteration $(k-1)$ which means $\hat{\boldsymbol{\theta}}_m^{k-1} = \boldsymbol{\theta}^{k-1}$, we can obtain

$$\|\nabla f_m(\hat{\boldsymbol{\theta}}_m^{k-1}) - \nabla f_m(\boldsymbol{\theta}^k)\|^2 \leq L_m^2 \|\hat{\boldsymbol{\theta}}_m^{k-1} - \boldsymbol{\theta}^k\|^2 \quad (79)$$

$$= L_m^2 \|\boldsymbol{\theta}^{k-1} - \boldsymbol{\theta}^k\|^2 \quad (80)$$

where (79) is obtained using the definition of the smoothness constant in Assumption 1.

If (20) is true, then $L_m^2 \|\boldsymbol{\theta}^{k-1} - \boldsymbol{\theta}^k\|^2$ can be bounded by $\varepsilon_1 \|\boldsymbol{\theta}^{k-1} - \boldsymbol{\theta}^k\|^2$. Thus, we have

$$\|\nabla f_m(\hat{\boldsymbol{\theta}}_m^{k-1}) - \nabla f_m(\boldsymbol{\theta}^k)\|^2 \leq \varepsilon_1 \|\boldsymbol{\theta}^{k-1} - \boldsymbol{\theta}^k\|^2 \quad (81)$$

which is equivalent to the CHB-skip-transmission condition in (8). The result in (81) indicates that worker m will not transmit at iteration k since the CHB-skip-transmission condition is satisfied. Thus, in the first k iterations, the worker m communicates with the server at most $k/2$ times if (20) holds.

REFERENCES

- [1] S. Liu, N. Gupta, and N. H. Vaidya, "Approximate byzantine fault-tolerance in distributed optimization," in *Proceedings of the 2021 ACM Symposium on Principles of Distributed Computing*, 2021, pp. 379–389.
- [2] B. Turan, C. A. Uribe, H.-T. Wai, and M. Alizadeh, "Robust distributed optimization with randomly corrupted gradients," *IEEE Transactions on Signal Processing*, 2022.
- [3] X. Li, L. Xie, and Y. Hong, "Distributed aggregative optimization over multi-agent networks," *IEEE Transactions on Automatic Control*, 2021.
- [4] Y. Zhang, Y. Lou, Y. Hong, and L. Xie, "Distributed projection-based algorithms for source localization in wireless sensor networks," *IEEE Transactions on Wireless Communications*, vol. 14, no. 6, pp. 3131–3142, 2015.
- [5] Y. Chen, R. S. Blum, B. M. Sadler, and J. Zhang, "Testing the structure of a gaussian graphical model with reduced transmissions in a distributed setting," *IEEE Transactions on Signal Processing*, vol. 67, no. 20, pp. 5391–5401, 2019.
- [6] Y. Chen, B. M. Sadler, and R. S. Blum, "Ordered transmission for efficient wireless autonomy," in *2018 52nd Asilomar Conference on Signals, Systems, and Computers*. IEEE, 2018, pp. 1299–1303.
- [7] Y. Chen, R. S. Blum, and B. M. Sadler, "Optimal quickest change detection in sensor networks using ordered transmissions," in *2020 IEEE 21st International Workshop on Signal Processing Advances in Wireless Communications (SPAWC)*. IEEE, 2020, pp. 1–5.
- [8] ———, "Ordering for communication-efficient quickest change detection in a decomposable graphical model," *IEEE Transactions on Signal Processing*, vol. 69, pp. 4710–4723, 2021.
- [9] G. Binetti, A. Davoudi, F. L. Lewis, D. Naso, and B. Turchiano, "Distributed consensus-based economic dispatch with transmission losses," *IEEE Transactions on Power Systems*, vol. 29, no. 4, pp. 1711–1720, 2014.
- [10] J. Park, S. Samarakoon, A. Elgabli, J. Kim, M. Bennis, S.-L. Kim, and M. Debbah, "Communication-efficient and distributed learning over wireless networks: Principles and applications," *Proceedings of the IEEE*, vol. 109, no. 5, pp. 796–819, 2021.
- [11] S. Vlaski and A. H. Sayed, "Distributed learning in non-convex environments—part i: Agreement at a linear rate," *IEEE Transactions on Signal Processing*, vol. 69, pp. 1242–1256, 2021.
- [12] A. Imteaj, U. Thakker, S. Wang, J. Li, and M. H. Amini, "A survey on federated learning for resource-constrained iot devices," *IEEE Internet of Things Journal*, vol. 9, no. 1, pp. 1–24, 2021.
- [13] Y. Chen, R. S. Blum, and B. M. Sadler, "Communication efficient federated learning via ordered admm in a fully decentralized setting," in *2022 56th Annual Conference on Information Sciences and Systems (CISS)*. IEEE, 2022, pp. 96–100.
- [14] V. Smith, S. Forte, C. Ma, M. Takáč, M. I. Jordan, and M. Jaggi, "Cocoa: A general framework for communication-efficient distributed optimization," *The Journal of Machine Learning Research*, vol. 18, no. 1, pp. 8590–8638, 2017.
- [15] Y. Chen, "Ordered transmissions, estimation, and parameter learning," Ph.D. dissertation, Lehigh University, 2021.
- [16] Y. Zhou, Q. Ye, and J. Lv, "Communication-efficient federated learning with compensated overlap-fedavg," *IEEE Transactions on Parallel and Distributed Systems*, vol. 33, no. 1, pp. 192–205, 2021.
- [17] E. Ozfatura, K. Ozfatura, and D. Gündüz, "Time-correlated sparsification for communication-efficient federated learning," in *2021 IEEE International Symposium on Information Theory (ISIT)*. IEEE, 2021, pp. 461–466.
- [18] D. Jhunjhunwala, A. Gadhikar, G. Joshi, and Y. C. Eldar, "Adaptive quantization of model updates for communication-efficient federated learning," in *ICASSP 2021-2021 IEEE International Conference on Acoustics, Speech and Signal Processing (ICASSP)*. IEEE, 2021, pp. 3110–3114.
- [19] C. Li, G. Li, and P. K. Varshney, "Communication-efficient federated learning based on compressed sensing," *IEEE Internet of Things Journal*, vol. 8, no. 20, pp. 15531–15541, 2021.
- [20] H. Gao, A. Xu, and H. Huang, "On the convergence of communication-efficient local sgd for federated learning," in *Proceedings of the AAAI Conference on Artificial Intelligence*, vol. 35, no. 9, 2021, pp. 7510–7518.
- [21] Y. Chen, R. S. Blum, M. Takáč, and B. M. Sadler, "Distributed learning with sparsified gradient differences," *IEEE Journal of Selected Topics in Signal Processing*, vol. 16, no. 3, pp. 585–600, 2022.
- [22] Y. Chen, B. M. Sadler, and R. S. Blum, "Ordered gradient approach for communication-efficient distributed learning," in *2020 IEEE 21st International Workshop on Signal Processing Advances in Wireless Communications (SPAWC)*. IEEE, 2020, pp. 1–5.
- [23] F. Sattler, A. Marban, R. Rischke, and W. Samek, "Cfd: Communication-efficient federated distillation via soft-label quantization and delta coding," *IEEE Transactions on Network Science and Engineering*, vol. 9, no. 4, pp. 2025–2038, 2021.
- [24] R. Höning, Y. Zhao, and R. Mullins, "Dadaquant: Doubly-adaptive quantization for communication-efficient federated learning," in *International Conference on Machine Learning*. PMLR, 2022, pp. 8852–8866.
- [25] X. Fan, Y. Wang, Y. Huo, and Z. Tian, "Communication-efficient federated learning through 1-bit compressive sensing and analog aggregation," in *2021 IEEE International Conference on Communications Workshops (ICC Workshops)*. IEEE, 2021, pp. 1–6.
- [26] Y. Wang, Y. Xu, Q. Shi, and T.-H. Chang, "Quantized federated learning under transmission delay and outage constraints," *IEEE Journal on Selected Areas in Communications*, vol. 40, no. 1, pp. 323–341, 2021.
- [27] A. R. Elkordy and A. S. Avestimehr, "Heterosag: Secure aggregation with heterogeneous quantization in federated learning," *IEEE Transactions on Communications*, vol. 70, no. 4, pp. 2372–2386, 2022.
- [28] S. Chen, C. Shen, L. Zhang, and Y. Tang, "Dynamic aggregation for heterogeneous quantization in federated learning," *IEEE Transactions on Wireless Communications*, vol. 20, no. 10, pp. 6804–6819, 2021.
- [29] A. Panda, S. Mahloujifar, A. N. Bhagoji, S. Chakraborty, and P. Mittal, "Sparsefed: Mitigating model poisoning attacks in federated learning with sparsification," in *International Conference on Artificial Intelligence and Statistics*. PMLR, 2022, pp. 7587–7624.
- [30] A. Mitra, R. Jaafar, G. J. Pappas, and H. Hassani, "Linear convergence in federated learning: Tackling client heterogeneity and sparse gradients," *Advances in Neural Information Processing Systems*, vol. 34, pp. 14606–14619, 2021.

[31] S. U. Stich, J.-B. Cordonnier, and M. Jaggi, "Sparsified sgd with memory," in *Advances in Neural Information Processing Systems*, 2018, pp. 4447–4458.

[32] M. Zinkevich, M. Weimer, L. Li, and A. J. Smola, "Parallelized stochastic gradient descent," in *Advances in neural information processing systems*, 2010, pp. 2595–2603.

[33] Y. Zhang, J. C. Duchi, and M. J. Wainwright, "Communication-efficient algorithms for statistical optimization," *The Journal of Machine Learning Research*, vol. 14, no. 1, pp. 3321–3363, 2013.

[34] R. McDonald, M. Mohri, N. Silberman, D. Walker, and G. S. Mann, "Efficient large-scale distributed training of conditional maximum entropy models," in *Advances in neural information processing systems*, 2009, pp. 1231–1239.

[35] H. B. McMahan, E. Moore, D. Ramage, and B. A. y Arcas, "Federated learning of deep networks using model averaging. corr abs/1602.05629 (2016)," *arXiv preprint arXiv:1602.05629*, 2016.

[36] O. Shamir, N. Srebro, and T. Zhang, "Communication-efficient distributed optimization using an approximate newton-type method," in *International conference on machine learning*, 2014, pp. 1000–1008.

[37] A. Agarwal, O. Chapelle, M. Dudík, and J. Langford, "A reliable effective terascale linear learning system," *The Journal of Machine Learning Research*, vol. 15, no. 1, pp. 1111–1133, 2014.

[38] A. Bordes, L. Bottou, and P. Gallinari, "Sgd-qn: Careful quasi-newton stochastic gradient descent," *Journal of Machine Learning Research*, vol. 10, no. Jul, pp. 1737–1754, 2009.

[39] R. H. Byrd, S. L. Hansen, J. Nocedal, and Y. Singer, "A stochastic quasi-newton method for large-scale optimization," *SIAM Journal on Optimization*, vol. 26, no. 2, pp. 1008–1031, 2016.

[40] P. Moritz, R. Nishihara, and M. Jordan, "A linearly-convergent stochastic l-bfgs algorithm," in *Artificial Intelligence and Statistics*, 2016, pp. 249–258.

[41] R. Gower, D. Goldfarb, and P. Richtárik, "Stochastic block bfgs: Squeezing more curvature out of data," in *International Conference on Machine Learning*, 2016, pp. 1869–1878.

[42] Y. Zhang and X. Lin, "Disco: Distributed optimization for self-concordant empirical loss," in *International conference on machine learning*, 2015, pp. 362–370.

[43] S. J. Reddi, J. Konečný, P. Richtárik, B. Póczos, and A. Smola, "Aide: Fast and communication efficient distributed optimization," *arXiv preprint arXiv:1608.06879*, 2016.

[44] J. C. Duchi, A. Agarwal, and M. J. Wainwright, "Dual averaging for distributed optimization: Convergence analysis and network scaling," *IEEE Transactions on Automatic control*, vol. 57, no. 3, pp. 592–606, 2011.

[45] K. Scaman, F. Bach, S. Bubeck, L. Massoulié, and Y. T. Lee, "Optimal algorithms for non-smooth distributed optimization in networks," in *Advances in Neural Information Processing Systems*, 2018, pp. 2740–2749.

[46] L. He, A. Bian, and M. Jaggi, "Cola: Decentralized linear learning," in *Advances in Neural Information Processing Systems*, 2018, pp. 4536–4546.

[47] C. Rago, P. Willett, and Y. Bar-Shalom, "Censoring sensors: A low-communication-rate scheme for distributed detection," *IEEE Transactions on Aerospace and Electronic Systems*, vol. 32, no. 2, pp. 554–568, 1996.

[48] S. Appadwedula, V. V. Veeravalli, and D. L. Jones, "Energy-efficient detection in sensor networks," *IEEE Journal on Selected areas in communications*, vol. 23, no. 4, pp. 693–702, 2005.

[49] S. Marano, V. Matta, P. Willett, and L. Tong, "Cross-layer design of sequential detectors in sensor networks," *IEEE Transactions on Signal Processing*, vol. 54, no. 11, pp. 4105–4117, 2006.

[50] N. Patwari, A. Hero, and B. M. Sadler, "Hierarchical censoring sensors for change detection," in *IEEE Workshop on Statistical Signal Processing, 2003.* IEEE, 2003, pp. 21–24.

[51] W. Chen and W. Ren, "Event-triggered zero-gradient-sum distributed consensus optimization over directed networks," *Automatica*, vol. 65, pp. 90–97, 2016.

[52] Q. Lü and H. Li, "Event-triggered discrete-time distributed consensus optimization over time-varying graphs," *Complexity*, vol. 2017, 2017.

[53] K. I. Tsianos, S. F. Lawlor, J. Y. Yu, and M. G. Rabbat, "Networked optimization with adaptive communication," in *2013 IEEE Global Conference on Signal and Information Processing*. IEEE, 2013, pp. 579–582.

[54] T. Chen, G. Giannakis, T. Sun, and W. Yin, "Lag: Lazily aggregated gradient for communication-efficient distributed learning," in *Advances in Neural Information Processing Systems*, 2018, pp. 5050–5060.

[55] T. K. Leen and G. B. Orr, "Optimal stochastic search and adaptive momentum," in *Advances in neural information processing systems*, 1994, pp. 477–484.

[56] I. Sutskever, J. Martens, G. Dahl, and G. Hinton, "On the importance of initialization and momentum in deep learning," in *International conference on machine learning*, 2013, pp. 1139–1147.

[57] L. Bottou, F. E. Curtis, and J. Nocedal, "Optimization methods for large-scale machine learning," *Siam Review*, vol. 60, no. 2, pp. 223–311, 2018.

[58] Y. Nesterov, *Lectures on convex optimization*. Springer, 2018, vol. 137.

[59] A. L. Peressini, F. E. Sullivan, and J. J. Uhl, *The mathematics of nonlinear programming*. Springer-Verlag New York, 1988.

[60] E. Ghadimi, H. R. Feyzmahdavian, and M. Johansson, "Global convergence of the heavy-ball method for convex optimization," *arXiv preprint arXiv:1412.7457*, 2014.

[61] A. Géron, *Hands-on machine learning with Scikit-Learn, Keras, and TensorFlow: Concepts, tools, and techniques to build intelligent systems*. O'Reilly Media, 2019.

[62] D. Prokhorov, "Ijcn 2001 neural network competition," *Slide presentation in IJCNN*, vol. 1, no. 97, p. 38, 2001.

[63] Y. LeCun, L. Bottou, Y. Bengio, and P. Haffner, "Gradient-based learning applied to document recognition," *Proceedings of the IEEE*, vol. 86, no. 11, pp. 2278–2324, 1998.